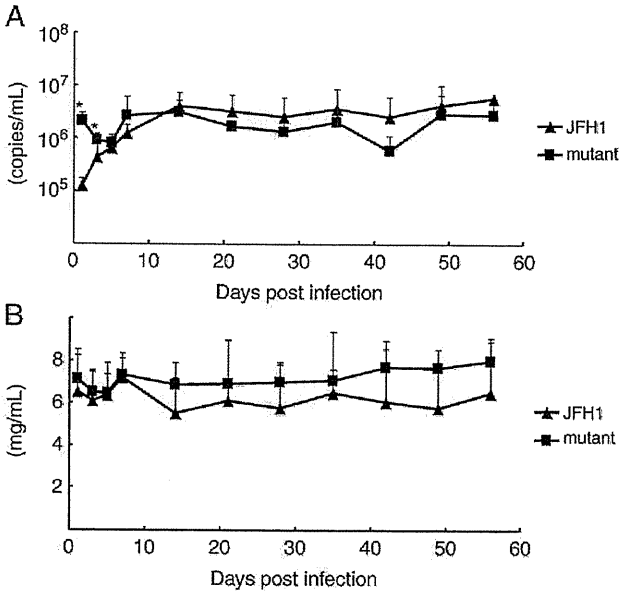

Fig. 6. In vivo analysis of cytopathic JFH1 mutants using human hepatocyte chimeric mice. A. Serial changes in HCV RNA in the sera of mice inoculated with the culture media from JFH1 mutants. The data shows the average of 2 mice for JFH1, and 3 mice for the mutant. Asterisks indicate p-values of less than 0.05 as compared with JFH1. B. Levels of human albumin in the sera of mice inoculated with the culture media from JFH1 mutants.

inoculated with the cytopathic mutant virus showed conservation of the mutations in codons 2441, 2938 and 2985. However, on days 21 and later, the mutation at codon 2985 had reverted to the wild type JFH1 sequence in all the mutant-injected mice and the mutation at codon 2938 had reverted to the wild type JFH1 sequence in two of the three mice. The C2441S mutation was more stable in the mutant-injected mice, but one mouse had lost it at day 56 (Fig. 8).

Discussion

In this study, we investigated the significance of genetic mutations in plaque-purified, cytopathic HCV-JFH1 subclones. Genetically engineered JFH1-mutants encoding C2441S, P2938S, and R2985P led to much more cell death than the wild type JFH1, and also produced significantly higher amounts of core antigen in the culture medium and inside the cells than the parental JFH1 clone. In the single-cycle production assay, which exploited a receptor-deficient Huh7 cell line, the three JFH1-mutants, JFH1-C2441S, P2938S, and R2985P produced significantly more core antigen in the culture medium and expressed equivalently higher amounts of viral genomic RNA in the cells. These data suggest that the three mutations in NS5A and NS5B (C2441S, P2938S, and R2985P) are associated directly with enhanced intracellular replication and resultant virion formation, which correlated with the extent of the cytopathic effects. Interestingly, inoculation of a cytopathogenic mutant, JFH1-C2441S/P2938S/R2985P, into human hepatocyte chimeric mice produced significantly higher plasma HCV RNA concentrations than JFH1 at ~7 days post inoculation. At a later phase of infection, however, the mutations in this mutant HCV reverted partially to the wild type sequences. Taking all things together, it is suggested that in vitro-isolated, genetically modified cytopathic HCV subclones replicate robustly in the acute phase of in vivo infection but are eliminated rapidly and substituted by in vivo adapted clones.

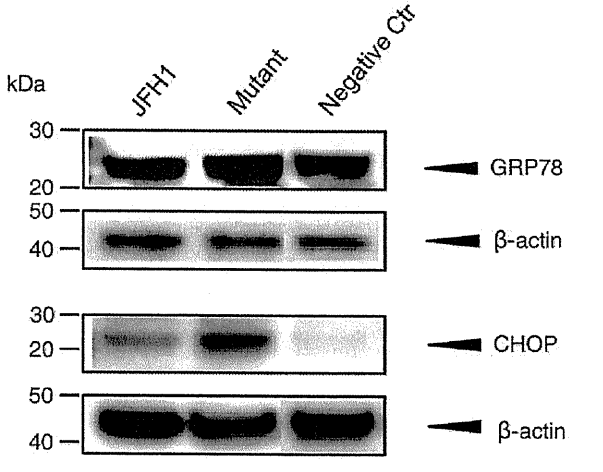

Fig. 7. Expression of ER stress-related proteins in human hepatocytes of chimeric mice infected with JFH1 or the mutant in the early phase. Western-blot analysis of the liver tissues of infected chimeric mice using anti-GRP78 goat monoclonal antibody, anti-GADD153/CHOP rabbit polyclonal antibody and anti-beta-actin. Liver samples were obtained at 5 days after inoculation. The negative control liver samples for this study was from uninfected human hepatocyte chimeric mouse.

Four of the five NS5B mutations appeared independently in several isolated subclones. This made us speculate that these amino acid substitutions may affect the enzymatic activity of RdRp. Mapping of the amino acid substitutions in the RdRp tertiary structure revealed that amino acid 2441 is located on the finger domain, and three amino acids, 2938, 2964, and 2985, are on the outer surface of the thumb domain, which corresponds to the opposite side of the nucleotide tunnel. The other substitutions, 3004 and 3005, are within the domain of the polypeptide linking the polymerase to the membrane anchor (Lesburg et al., 1999). Our preliminary study has shown that the NS5B mutations, P2938S and R2985P, did not affect cell-free enzymatic activities of the RNA polymerase. Thus, it is speculated that these mutations may affect the stability of the HCV replicase complex by altering surface affinity to other nonstructural proteins.

There are several reports on cell culture adaptive mutations in the HCV-JFH1 genome that gave more vigorous and consistent virus expression. Most studies involved prolonged cell culture of HCV-JFH1 or multiple rounds of successive passage onto naïve cells. Zhong et al. detected the E2-G451R mutation after culture for more than 60 days. The mutation led to more efficient production of infectious viral particles than wild type JFH1 (Zhong et al., 2006). Delgrange et al. conducted successive virus infections of naïve cells and identified the E2-N534K mutation that facilitated virus-CD81 attachment, and core-F172C and -P173S that increased secretion of virions (Delgrange et al., 2007). Using a similar method, Russell et al. identified E2-N417S that improved virus–cell attachment, and p7-N765D and NS2-Q1012R that increased virion production (Russell et al., 2008). Kaul et al. reported the NS5A-V2440L mutation, that was close to the C terminus and increased virion production (Kaul et al., 2007). Yi et al. used a chimeric virus of genotype 1a and JFH1 and identified the NS3-Q1251L mutation that resulted in enhanced virus production, possibly through improved interactions between NS2 and NS3 that were required for virion formation (Yi et al., 2002). Han et al. used EGFP-tagged virus and identified the mutually dependent mutations, NS3-M1290K and NS5A-T2438I, which improved virus production synergistically (Han et al., 2009).

Of note is that all of the mutations reported above promoted virion secretion or virus–cell surface interaction and none of them showed any effect on intracellular replication of viral RNA or translation of virus proteins. None of the adaptive mutations reported above overlapped with our cytopathogenic mutations. The mutations that we have identified conferred enhanced virus replication and protein expression in the early/acute stages of infection and subsequently led to massive cell death. Our data and the reports of other groups suggest that the HCV genome evolves to adapt to the host cell environment. Mutations that optimize virus secretion or virus–cell entry may be

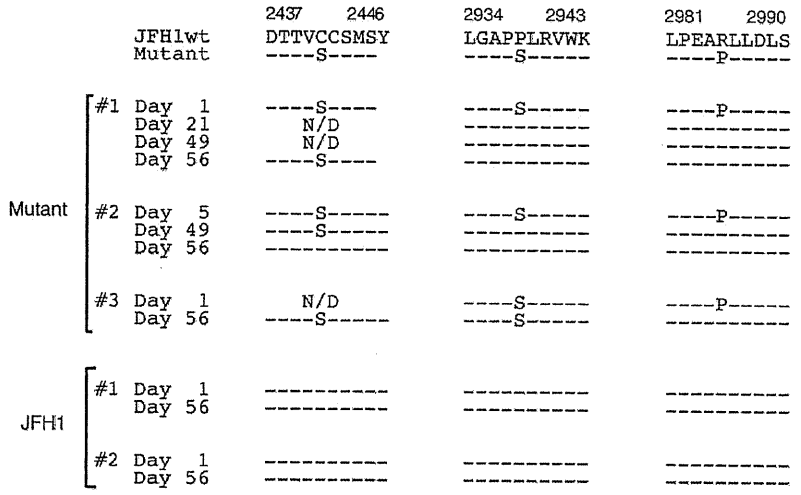

Fig. 8. Nucleotide sequence analysis of virus genomes circulating in the sera of infected mice. We extracted RNA from the sera of mice inoculated with culture media from JFH1 or JFH1-mutants and analyzed the viral sequence at the specified time points. N/D is not detectable. Wt: Wild type.

required for persistent infection in vitro, while those that affect cellular viral RNA replication may possibly promote viral genetic evolution and host cell damage.

The results of in vivo experiments using human hepatocyte chimeric mice were consistent with those of virus cell culture (Figs. 5, 6 and 7). The mutant JFH1 clones showed markedly higher levels of replication than the parental JFH1 in the acute phases. However, the serum HCV titers subsequently leveled out after two weeks of infection, concomitant with reversal of some cytopathic mutations to wild type sequences. Bukh et al. reported that inoculation of the HCV-1b genome into chimpanzee liver resulted in persistent infection, although the mutation reverted rapidly to wild type (Bukh et al., 2002). In this study, the NS5A-C2441S mutation was preserved in 2 of 3 mice, while NS5B-P2938S reverted to the wild type sequences in 2 of 3 mice and NS5B-R2985P reverted to wild type sequences in all 3 mice. These results suggest that the highly adapted JFH1 genome is infectious and viable in vivo, but is not as fit in vitro.

It is not clear why the subgenomic replicons with C2441S, P2938S or R2985P mutations did not show differences in replication levels compared to the wild type JFH1 subgenomic replicon. One may speculate that this discrepancy between the results using full-length HCV genomes and replicons might be the presence or absence of the HCV structural proteins. In addition, three individual substitutions G2964D, H3004Q and S3005N did not enhance viral replication as compared with the parental JFH1 nor did express detectable amounts of core protein. It is speculated that these mutants exist in host cells through co-infection with replication-competent viral clones resulting in enhanced replication.

There is clinical evidence that suggests the pathological outcomes of hepatitis C result from the immune response of the host rather than the direct cytopathic effects of the virus (Cerny and Chisari, 1999). However, several clinical studies have shown that fulminant hepatic failure (FHF, the HCV-JFH1 strain was isolated from such a case) featured massive hepatocyte apoptosis, as characterized by caspase activation and Fas–FasL expression (Leifeld et al., 2006; Mita et al., 2005; Ryo et al., 2000). The ER stress markers, GRP78 and ATF6 are upregulated in HCV-infected liver tissue as the histological grade advances (Shuda et al., 2003). This background and our results in vitro and in vivo suggest that HCV strains with highly infectious and cytopathic gene signatures may replicate aggressively in the acute phase of infection and that certain defects in innate or adaptive immune responses against the virus could lead to severe and persistent liver damage due to cytopathic effects induced directly by HCV. Such mechanisms might explain some rare clinical features of HCV infection, such as fulminant hepatic failure and post-transplantation severe fibrosing cholestatic hepatitis (Delladetsima et al., 1999; Dixon and Crawford, 2007).

In conclusion, we identified three substitutions in cytopathic HCV-JFH1 subclones derived from plaque assay. These substitutions directly enhanced virus replication in the early phases of virus infection in vitro and in vivo. This highly enhanced replication induced ER stress-mediated apoptosis and resulted in cytopathogenicity. Further analyses of cellular effects on HCV replication may elucidate the pathogenesis of HCV infection and may define novel host factors as targets of antiviral chemotherapeutics.

Materials and methods

Cells and cell culture

Huh-7.5.1 cells (Zhong et al., 2005) (kindly provided by Dr Francis V. Chisari) and CD81 deficient Huh7-S29 cells (Russell et al., 2008) (kindly provided by Dr Rodney S. Russell and Dr Robert H. Purcell) were maintained in Dulbecco's modified minimal essential medium (DMEM, Sigma, St. Louis, MO) supplemented with 2 mmol/L L-glutamine and 10% fetal bovine serum at 37 °C under 5.0% CO_2.

Sequence analysis

The cDNA from the isolated JFH1-plaque was amplified from cytopathic virus-infected Huh-7.5.1 cells by RT-PCR and subjected to direct sequencing.

In vitro RNA synthesis and transfection

A plasmid, pJFH1full (Wakita et al., 2005), which encodes full-length HCV-JFH1 sequence, was used. In vitro RNA synthesis and transfection were conducted as previously described (Sekine-Osajima et al., 2008). Briefly, HCV RNA was synthesized from linearized pJFH1 plasmid as template and transfected into Huh-7.5.1 cells by electroporation. The transfected cells were split every 3 to 5 days. The culture media were subsequently transferred onto uninfected Huh-7.5.1 cells and Huh7-S29 cells. The levels of HCV replication and viral protein expression were detected by real-time PCR and western blotting.

Plaque assay

HCV plaque assays were performed as reported previously (Sekine-Osajima et al., 2008). Huh-7.5.1 cells were seeded in collagen-coated 60 mm-diameter plates. After overnight incubation, HCV-infected culture media were serially diluted in a final volume of 2 ml per plate and transferred onto the cell monolayer. After ~5 h of incubation, the inocula were removed and the cell monolayer was overlaid with 8 ml of culture medium containing 0.8% methylcellulose (Sigma). After 7 to 12 days culture, cytopathic plaques were visualized by staining with 0.08% crystal violet solution (Sigma). The levels of cytotoxicity were evaluated by counting the plaques and calculating the titer (plaque-forming unit/ml).

Establishment of mutant JFH1 clones

In order to introduce various mutations into the NS5A and NS5B region of JFH1, plasmid pJFH1 was digested with HindIII and the DNA fragment encompassing nt. 8231 to 9731 was subcloned into the pBluescript II SK+ phagemid vector (Stratagene, La Jolla, CA). Mutations were introduced into the DNA fragment in the subcloning vector by site-directed mutagenesis (Quick-ChangeII Site-Directed Mutagenesis Kit, Stratagene) to generate the following codon changes: P2938S, G2964D, R2985P, H3004Q and S3005N. Finally, the HindIII–HindIII fragments were subcloned back into the parental plasmid, pJFH1. A PCR fragment (nt. 7421–7839) was subcloned into the pGEM-T Easy plasmid vector (Promega, Madison, WI) and digested with RsrII and BsrGI. Finally, after introducing the codon change C2441S, the RsrII–BsrGI fragment was reinserted into the parental plasmid.

Quantification of HCV core antigen in the culture medium

The culture media from JFH1-RNA transfected Huh-7.5.1 cells and Huh7-S29 cells were collected on the days indicated, passed through a 0.45 μm filter (MILLEX-HA, Millipore, Bedford, MA), and stored at −80 °C. The levels of core antigen in the culture media were measured using a chemiluminescence enzyme immunoassay (CLEIA) according to the manufacturer's protocol (Lumipulse Ortho HCV Antigen, Ortho-Clinical Diagnostics, Tokyo, Japan).

Western blotting

Western blotting was carried out as described previously (Itsui et al., 2009). Briefly, 10 μg of total cell lysate were separated by SDS-PAGE and blotted onto a polyvinylidene fluoride (PVDF) Western Blotting membrane. The membrane was incubated with the primary antibodies followed by a peroxidase-labeled anti IgG antibody, and visualized by chemiluminescence using the ECL Western blotting Analysis System (Amersham Bioscience, Buckinghamshire, UK). The antibodies used were anti-core mouse monoclonal antibody (Abcam, Cambridge, MA), anti-GRP78 goat monoclonal antibody, anti-GADD153/CHOP rabbit polyclonal antibody (Santa Cruz Biotechnology, Santa Cruz, CA), and anti-beta-actin antibody (Sigma).

HCV subgenomic replicon constructs

The HCV subgenomic replicon plasmid, pRep-Feo, was derived from the HCV-N strain, pHCV1bneo-delS (Tanabe et al., 2004; Yokota et al., 2003). The replicon RNA was synthesized from pRep-Feo and transfected into Huh7 cells.

Luciferase reporter assay

Luciferase activity was measured using a 1420 Multilabel Counter (ARVO MX, Perkin Elmer, Waltham, MA) with a Bright-Glo Luciferase Assay System (Promega) (Tasaka et al., 2007). Assays were carried out in triplicate and the results expressed as means ± SD.

MTS assays

To evaluate cell viability, dimethylthiazol carboxymethoxy-phenyl sulfophenyl tetrazolium (MTS) assays were performed using a CellTiter 96 Aqueous One Solution Cell Proliferation Assay kit (Promega), as described previously (Sakamoto et al., 2007).

Real-time RT-PCR analysis

Total cellular RNA was isolated using an RNeasy Mini Kit (QIAGEN, Valencia, CA). Two micro-grams of total cellular RNA were used to generate cDNA from each sample using SuperScript II (Invitrogen) reverse transcriptase. Expression of mRNA was quantified using TaqMan Universal PCR Master Mix (Applied Biosystems) and the ABI 7500 Real-Time PCR System (Applied Biosystems). The primers used were as follows: HCV-JFH1 sense (positions 285 to 307; 5′-GGT-ACTGCCTGATAGGGTGCTT-3′), HCV-JFH1 antisense (positions 349 to 375; 5′-TGGTTTTTCTTTGAGGTTTAGGATTC-3′), GAPDH sense (5′-CCTCCCGCTTCGCTCTCT-3′), and GAPDH antisense (5′-GCTGGCGACG-CAAAAGA-3′).

HCV RNA inoculation into human hepatocyte chimeric mice

Housing, maintenance, and care of the mice used in this study conformed to the requirement for the humane use of animals in scientific research as defined by Animal Care and Use Committee of our institute. The culture media of Huh-7.5.1 cells transfected with parental JFH1 and JFH1 mutants were collected 10 days after transfection and passed through a 0.45 μm filter. The three mutations introduced in NS5A and NS5B were confirmed to conserve by the sequence analysis of virus genome of cell culture supernatants before inoculation. Filtrated culture medium was then pooled and concentrated using Amicon Ultra-15 (100,000 molecular weight cutoff, Millipore). 100 μl of each culture medium was injected intravenously into human hepatocyte chimeric mice (PXB mice, Phenix Bio, Hiroshima, Japan) (Mercer et al., 2001). The rate of liver chimerism of these human hepatocyte chimeric mice was confirmed more than 70% by immunohistochemical analysis. After infection, blood samples were taken serially and levels for HCV RNA and human albumin were quantified using real-time RT-PCR and an enzyme immunoassay, respectively. RNA was extracted from serum samples and subjected to direct sequence determination.

Protein extraction from human hepatocyte chimeric mice and expression of ER stress-related proteins

5 days post inoculation, mice were sacrificed and proteins were extracted from liver samples with complete Lysis-M Reagent Kit (Roche Applied Science, Indianapolis, IN). One Mini Protease Inhibitor Cocktail Tablet was dissolved into 10 ml of Lysis-M Reagent and 500 μl of this fluid was added to 50 μg of each liver sample and homogenized. The lysate was transferred to a microcentrifuge tube and centrifuged at 14,000×*g* for 5 min. The supernatant containing soluble protein was transferred to a new reaction tube and 20 μg of each protein was used for western blotting to detect ER stress-related proteins.

Acknowledgments

We are indebted to Dr. Francis V. Chisari for providing the Huh-7.5.1 cell line and Dr. Rodney S. Russell for receptor-deficient Huh7-S29 cells. This study was supported by grants from Ministry of Education, Culture, Sports, Science and Technology-Japan, the Japan Society for the Promotion of Science, Ministry of Health, Labour and

Welfare-Japan, Japan Health Sciences Foundation, and National Institute of Biomedical Innovation.

References

Alter, M.J., 1997. Epidemiology of hepatitis C. Hepatology 26, 62S–65S.

Bartenschlager, R., Lohmann, V., 2000. Replication of hepatitis C virus. J. Gen. Virol. 81, 1631–1648.

Bukh, J., Pietschmann, T., Lohmann, V., Krieger, N., Faulk, K., Engle, R.E., Govindarajan, S., Shapiro, M., Claire, M.S., Bartenschlager, R., 2002. Mutations that permit efficient replication of hepatitis C virus RNA in Huh-7 cells prevent productive replication in chimpanzees. Proc. Natl. Acad. Sci. U. S. A. 99 (22), 14416–14421.

Cerny, A., Chisari, F.V., 1999. Pathogenesis of chronic hepatitis C: immunological features of hepatic injury and viral persistence. Hepatology 30 (3), 595–601.

Delgrange, D., Pillez, A., Castelain, S., Cocquerel, L., Rouille, Y., Dubuisson, J., Wakita, T., Duverlie, G., Wychowski, C., 2007. Robust production of infectious viral particles in Huh-7 cells by introducing mutations in hepatitis C virus structural proteins. J. Gen. Virol. 88 (Pt 9), 2495–2503.

Delladetsima, J.K., Boletis, J.N., Makris, F., Psichogiou, M., Kostakis, A., Hatzakis, A., 1999. Fibrosing cholestatic hepatitis in renal transplant recipients with hepatitis C virus infection. Liver Transpl. Surg. 5 (4), 294–300.

Dixon, L.R., Crawford, J.M., 2007. Early histologic changes in fibrosing cholestatic hepatitis C. Liver Transpl. 13 (2), 219–226.

Fried, M.W., Shiffman, M.L., Reddy, K.R., Smith, C., Marionos, G., Goncales, F.L., Häussinger, D., Diago, M., Garosi, G., Dhumeaux, D., Craxi, A., Lin, A., Hoffman, J., Yu, J., 2002. Peginterferon alfa-2a plus ribavirin for chronic hepatitis C virus infection. N. Engl. J. Med. 347, 975–982.

Han, Q., Xu, C., Wu, C., Zhu, W., Yang, R., Chen, X., 2009. Compensatory mutations in NS3 and NS5A proteins enhance the virus production capability of hepatitis C reporter virus. Virus Res. 145 (1), 63–73.

Itsui, Y., Sakamoto, N., Kakinuma, S., Nakagawa, M., Sekine-Osajima, Y., Tasaka-Fujita, M., Nishimura-Sakurai, Y., Suda, G., Karakama, Y., Yamamoto, M., Watanabe, T., Ueyama, M., Funaoka, Y., Azuma, S., and Watanabe, M. (2009). Antiviral effects of the interferon-induced protein GBP-1 and its interaction with the hepatitis C virus NS5B protein. Hepatology 50 (6), 1727–1737.

Jordan, R., Wang, L., Graczyk, T.M., Block, T.M., Romano, P.R., 2002. Replication of a cytopathic strain of bovine viral diarrhea virus activates PERK and induces endoplasmic reticulum stress-mediated apoptosis of MDBK cells. J. Virol. 76 (19), 9588–9599.

Kato, N., 2001. Molecular virology of hepatitis C virus. Acta Med. Okayama 55 (3), 133–159.

Kato, T., Date, T., Miyamoto, M., Furusaka, A., Tokushige, K., Mizokami, M., Wakita, T., 2003. Efficient replication of the genotype 2a hepatitis C virus subgenomic replicon. Gastroenterology 125 (6), 1808–1817.

Kaul, A., Woerz, I., Meuleman, P., Leroux-Roels, G., Bartenschlager, R., 2007. Cell culture adaptation of hepatitis C virus and in vivo viability of an adapted variant. J. Virol. 81 (23), 13168–13179.

Koutsoudakis, G., Herrmann, E., Kallis, S., Bartenschlager, R., Pietschmann, T., 2007. The level of CD81 cell surface expression is a key determinant for productive entry of hepatitis C virus into host cells. J. Virol. 81 (2), 588–598.

Leifeld, L., Nattermann, J., Fielenbach, M., Schmitz, V., Sauerbruch, T., Spengler, U., 2006. Intrahepatic activation of caspases in human fulminant hepatic failure. Liver Int. 26 (7), 872–879.

Lesburg, C.A., Cable, M.B., Ferrari, E., Hong, Z., Mannarino, A.F., Weber, P.C., 1999. Crystal structure of the RNA-dependent RNA polymerase from hepatitis C virus reveals a fully encircled active site. Nat. Struct. Biol. 6 (10), 937–943.

Lindenbach, B.D., Evans, M.J., Syder, A.J., Wolk, B., Tellinghuisen, T.L., Liu, C.C., Maruyama, T., Hynes, R.O., Burton, D.R., McKeating, J.A., Rice, C.M., 2005. Complete replication of hepatitis C virus in cell culture. Science 309 (5734), 623–626.

Lohmann, V., Korner, F., Koch, J., Herian, U., Theilmann, L., Bartenschlager, R., 1999. Replication of subgenomic hepatitis C virus RNAs in a hepatoma cell line. Science 285 (5424), 110–113.

Mercer, D.F., Schiller, D.E., Elliott, J.F., Douglas, D.N., Hao, C., Rinfret, A., Addison, W.R., Fischer, K.P., Churchill, T.A., Lakey, J.R., Tyrrell, D.L., Kneteman, N.M., 2001. Hepatitis C virus replication in mice with chimeric human livers. Nat. Med. 7 (8), 927–933.

Mita, A., Hashikura, Y., Tagawa, Y., Nakayama, J., Kawakubo, M., Miyagawa, S., 2005. Expression of Fas ligand by hepatic macrophages in patients with fulminant hepatic failure. Am. J. Gastroenterol. 100 (11), 2551–2559.

Mottola, G., Cardinali, G., Ceccacci, A., Trozzi, C., Bartholomew, L., Torrisi, M.R., Pedrazzini, E., Bonatti, S., Migliaccio, G., 2002. Hepatitis C virus nonstructural proteins are localized in a modified endoplasmic reticulum of cells expressing viral subgenomic replicons. Virology 293 (1), 31–43.

Russell, R.S., Meunier, J.C., Takikawa, S., Faulk, K., Engle, R.E., Bukh, J., Purcell, R.H., Emerson, S.U., 2008. Advantages of a single-cycle production assay to study cell culture-adaptive mutations of hepatitis C virus. Proc. Natl. Acad. Sci. U. S. A. 105 (11), 4370–4375.

Ryo, K., Kamogawa, Y., Ikeda, I., Yamauchi, K., Yonehara, S., Nagata, S., Hayashi, N., 2000. Significance of Fas antigen-mediated apoptosis in human fulminant hepatic failure. Am. J. Gastroenterol. 95 (8), 2047–2055.

Sakamoto, N., Watanabe, M., 2009. New therapeutic approaches to hepatitis C virus. J. Gastroenterol. 44 (7), 643–649.

Sakamoto, N., Yoshimura, M., Kimura, T., Toyama, K., Sekine-Osajima, Y., Watanabe, M., Muramatsu, M., 2007. Bone morphogenetic protein-7 and interferon-alpha synergistically suppress hepatitis C virus replicon. Biochem. Biophys. Res. Commun. 357 (2), 467–473.

Sekine-Osajima, Y., Sakamoto, N., Mishima, K., Nakagawa, M., Itsui, Y., Tasaka, M., Nishimura-Sakurai, Y., Chen, C.H., Kanai, T., Tsuchiya, K., Wakita, T., Enomoto, N., Watanabe, M., 2008. Development of plaque assays for hepatitis C virus-JFH1 strain and isolation of mutants with enhanced cytopathogenicity and replication capacity. Virology 371 (1), 71–85.

Shuda, M., Kondoh, N., Imazeki, N., Tanaka, K., Okada, T., Mori, K., Hada, A., Arai, M., Wakatsuki, T., Matsubara, O., Yamamoto, N., Yamamoto, M., 2003. Activation of the ATF6, XBP1 and grp78 genes in human hepatocellular carcinoma: a possible involvement of the ER stress pathway in hepatocarcinogenesis. J. Hepatol. 38 (5), 605–614.

Tanabe, Y., Sakamoto, N., Enomoto, N., Kurosaki, M., Ueda, E., Maekawa, S., Yamashiro, T., Nakagawa, M., Chen, C.H., Kanazawa, N., Watanabe, M., 2004. Synergistic inhibition of intracellular hepatitis C virus replication by combination of ribavirin and interferon-alpha. J. Infect. Dis. 189, 1129–1139.

Tasaka, M., Sakamoto, N., Itakura, Y., Nakagawa, M., Itsui, Y., Sekine-Osajima, Y., Nishimura-Sakurai, Y., Chen, C.H., Yoneyama, M., Fujita, T., Wakita, T., Maekawa, S., Enomoto, N., Watanabe, M., 2007. Hepatitis C virus non-structural proteins responsible for suppression of the RIG-I/Cardif-induced interferon response. J. Gen. Virol. 88 (Pt 12), 3323–3333.

Wakita, T., Pietschmann, T., Kato, T., Date, T., Miyamoto, M., Zhao, Z., Murthy, K., Habermann, A., Krausslich, H.G., Mizokami, M., Bartenschlager, R., Liang, T.J., 2005. Production of infectious hepatitis C virus in tissue culture from a cloned viral genome. Nat. Med. 11 (7), 791–796.

Yi, M., Bodola, F., Lemon, S.M., 2002. Subgenomic hepatitis C virus replicons inducing expression of a secreted enzymatic reporter protein. Virology 304 (2), 197–210.

Yokota, T., Sakamoto, N., Enomoto, N., Tanabe, Y., Miyagishi, M., Maekawa, S., Yi, L., Kurosaki, M., Taira, K., Watanabe, M., Mizusawa, H., 2003. Inhibition of intracellular hepatitis C virus replication by synthetic and vector-derived small interfering RNAs. EMBO Rep. 4 (6), 602–608.

Zhong, J., Gastaminza, P., Cheng, G., Kapadia, S., Kato, T., Burton, D.R., Wieland, S.F., Uprichard, S.L., Wakita, T., Chisari, F.V., 2005. Robust hepatitis C virus infection in vitro. Proc. Natl. Acad. Sci. U. S. A. 102 (26), 9294–9299.

Zhong, J., Gastaminza, P., Chung, J., Stamataki, Z., Isogawa, M., Cheng, G., McKeating, J.A., Chisari, F.V., 2006. Persistent hepatitis C virus infection in vitro: coevolution of virus and host. J. Virol. 80 (22), 11082–11093.

Journal of General Virology (2010), **91**, 1668–1677 DOI 10.1099/vir.0.019315-0

Practical evaluation of a mouse with chimeric human liver model for hepatitis C virus infection using an NS3-4A protease inhibitor

Naohiro Kamiya,[1] Eiji Iwao,[1] Nobuhiko Hiraga,[2,3] Masataka Tsuge,[2,3] Michio Imamura,[2,3] Shoichi Takahashi,[2,3] Shinji Miyoshi,[4] Chise Tateno,[3,5] Katsutoshi Yoshizato[3,5] and Kazuaki Chayama[2,3]

Correspondence
Kazuaki Chayama
chayama@hiroshima-u.ac.jp

[1]Pharmacology Department V, Mitsubishi Tanabe Pharma Corporation, Yokohama, Japan

[2]Department of Medicine and Molecular Science, Division of Frontier Medical Science, Programs for Biomedical Research, Graduate School of Biomedical Sciences, Hiroshima University, Hiroshima, Japan

[3]Liver Research Project Center, Hiroshima University, Hiroshima, Japan

[4]DMPK Department, Mitsubishi Tanabe Pharma Corporation, Kisarazu, Chiba, Japan

[5]PhoenixBio, Higashihiroshima, Japan

Received 17 December 2009
Accepted 17 February 2010

A small-animal model for hepatitis C virus (HCV) infection was developed using severe combined immunodeficiency (SCID) mice encoding homozygous urokinase-type plasminogen activator (uPA) transplanted with human hepatocytes. Currently, limited information is available concerning the HCV clearance rate in the SCID mouse model and the virion production rate in engrafted hepatocytes. In this study, several cohorts of $uPA^{+/+}/SCID^{+/+}$ mice with nearly half of their livers repopulated by human hepatocytes were infected with HCV genotype 1b and used to evaluate HCV dynamics by pharmacokinetic and pharmacodynamic analyses of a specific NS3-4A protease inhibitor (telaprevir). A dose-dependent reduction in serum HCV RNA was observed. At telaprevir exposure equivalent to that in clinical studies, rapid turnover of serum HCV was also observed in this mouse model and the estimated slopes of virus decline were 0.11–0.17 $\log_{10}$ h^{-1}. During the initial phase of treatment, the $\log_{10}$ reduction level of HCV RNA was dependent on the drug concentration, which was about fourfold higher in the liver than in plasma. HCV RNA levels in the liver relative to human endogenous gene expression were correlated with serum HCV RNA levels at the end of treatment for up to 10 days. A mathematical model analysis of viral kinetics suggested that 1 g of the chimeric human liver could produce at least 10^8 virions per day, and this may be comparable to HCV production in the human liver.

INTRODUCTION

Hepatitis C virus (HCV) is a major cause for concern worldwide. More than 3 % of the world's population is chronically infected with HCV and 3–4 million people are newly infected each year (Wasley & Alter, 2000). Chronic HCV infection is relatively mild and progresses slowly; however, about 20 % of chronic hepatitis C (CHC) carriers progress to serious end-stage liver disease (Lauer & Walker, 2001; Liang *et al.*, 2000; Poynard *et al.*, 2003). The current standard treatment for HCV infection is administration of pegylated alpha interferon (PEG-IFN) in combination with ribavirin (RBV) for 48 weeks. The overall cure rates with this intervention are 40–50 % for patients with genotype 1 and more than 75 % for patients with genotypes 2 and 3 (Fried *et al.*, 2002; Manns *et al.*, 2001). Several compounds that inhibit specific stages of the virus life cycle have been clinically evaluated (Manns *et al.*, 2007; Pereira & Jacobson, 2009). Telaprevir is a novel peptidomimetic slow- and tight-binding inhibitor of HCV NS3-4A protease, which was discovered using a structure-based drug design approach (Perni *et al.*, 2006). A rapid decline in viral RNA was observed in CHC patients treated with telaprevir (Reesink *et al.*, 2006) and an increased antiviral effect of a combination of telaprevir and PEG-IFN has been reported (Forestier *et al.*, 2007). Recent clinical trials of telaprevir in combination with PEG-IFN and RBV have indicated a promising material advance in therapy for CHC patients (Hézode *et al.*, 2009; McHutchison *et al.*, 2009). First-generation HCV-specific agents have been developed despite the lack of small-animal models for HCV infection. However, early emergence of resistant variants against novel antiviral agents is a concern. Thus, the use of two or more investigation agents is strongly recommended for

clinical studies in CHC patients (Sherman *et al.*, 2007). To ensure ethical and safe clinical trials, animal models continue to be necessary for the mechanistic evaluation of the ability of specific agents to inhibit the virus life cycle *in vivo* and to develop better therapeutic strategies, including combination regimens (Boonstra *et al.*, 2009). Several groups have developed a small-animal model for HCV infection using homozygous urokinase-type plasminogen activator (uPA)/severe combined immunodeficiency (SCID) ($uPA^{+/+}/SCID^{+/+}$) mice transplanted with human hepatocytes (Mercer *et al.*, 2001). These mice are susceptible to cell culture-grown HCV (HCVcc; Lindenbach *et al.*, 2006) and have been used to evaluate antiviral agents including IFN-α, BILN 2061 (an NS3-4A protease inhibitor) and HCV796 (an NS5B polymerase inhibitor) (Kneteman *et al.*, 2006, 2009; Vanwolleghem *et al.*, 2007). However, the HCV clearance rate in the SCID mouse model and the virion production rate in hepatocytes engrafted in the mouse liver are not fully understood. We also generated a mouse model with an almost humanized liver (Tateno *et al.*, 2004). Using this mouse model, we reported the infection of a genetically engineered hepatitis B virus (Tsuge *et al.*, 2005) and developed a reverse genetics system for HCV genotypes 1a, 1b and 2a after intrahepatic injection of *in vitro*-transcribed RNA as well as intravenous injection of HCVcc (Hiraga *et al.*, 2007; Kimura *et al.*, 2008). In this study, we demonstrated the rapid turnover of serum HCV RNA and the pharmacokinetics (PK) and pharmacodynamics (PD) of telaprevir treatment. We concluded after quantitative estimation and the use of a mathematical model that HCV production equivalent to that in the human liver is possible in engrafted hepatocytes in this mouse model.

RESULTS

Preliminary dose-finding study

At the beginning of this study, we attempted to determine an effective dose regimen for telaprevir in this mouse model. Nine mice were randomized and treated with telaprevir over three time periods (Table 1). The lifetime kinetics of serum HCV RNA and of human serum albumin (HSA) in blood are represented in Fig. 1. One mouse (A07) exhibited a rapid reduction in HSA in the blood, which indicated the instability of human hepatocyte grafts. As a rapid reduction in HSA levels was not observed in subsequent experiments, this mouse was excluded from the mean analysis. After 7 days of twice daily (BID) dosing in period 1, the mean $\log_{10}$ changes in HCV RNA from baseline ($\pm$SEM) after the 100 and 10 mg telaprevir kg^{-1} doses were -0.49 ± 0.094 and -0.53 ± 0.039, respectively, and no dose-dependent reduction was observed. During period 2, the dose frequency was changed from BID to three times daily (TID), and the time of serum sampling was also changed from 1 to 4 h after the last dose. After the 3-day treatment, the mean $\log_{10}$ changes of HCV RNA in 100 and 10 mg telaprevir kg^{-1} TID groups were -1.00 ± 0.166 and -0.28 ± 0.056, respectively, and the difference between the two groups was significant. To test the reproducibility of results, mice were treated with 10 or 100 mg telaprevir kg^{-1} TID for 10 days and then sacrificed 5 h after the administration of the last dose. The mean $\log_{10}$ changes in serum HCV RNA were -1.46 ± 0.265 and -0.27 ± 0.073 in the 100 and 10 mg kg^{-1} TID groups, respectively, and the difference between the means was significant.

Evaluation of HCV turnover in this mouse model

Because of the SCID nature of this mouse model, the virion clearance mechanism was of interest. Six mice with steady-state and high viral loads (9.7×10^5–1.2×10^8 copies ml^{-1}) were administered 200 mg telaprevir kg^{-1} TID for 4 days, with 5 h intervals between doses and a 14 h intermission from drug treatment each day. Because the $\log_{10}$ reduction in HCV RNA appeared to depend on the time of serum collection during the day (Fig. 2a), the mean $\log_{10}$ changes in HCV RNA were plotted against time and fitted to a linear regression model (Fig. 2b). The estimated slopes (i.e. $\log_{10}$ HCV reduction per hour) and 95% confidence intervals (CI) on days 1, 2 and 3 were -0.165 (-0.268 to 0.0616), -0.115 (-0.131 to 0.0990) and -0.153, respectively. These regression lines also suggested that extrapolated HCV loads at the actual times of the daily first doses were 0.0530, -0.220 and -0.0948 $\log_{10}$ copies ml^{-1}, respectively. Therefore, it appeared that the viral load

Table 1. Telaprevir dose-finding experiment

Period	Duration (days)	Frequency of dose (per day)	Dose (mg kg^{-1})	No. of mice	Mean $\log_{10}$ changes $\pm$ SEM	*P* value (*t* test)
1	7	2	100	4	-0.49 ± 0.094	0.7806
			10	3*	-0.53 ± 0.039	
			0	1	-0.47	
2	3	3	100	4*	-1.00 ± 0.166	0.0064
			10	4	-0.28 ± 0.056	
3	10	3	100	3	-1.46 ± 0.265	0.0125
			10	3	-0.27 ± 0.073	

*One mouse was excluded because of instability of human hepatocyte grafts.

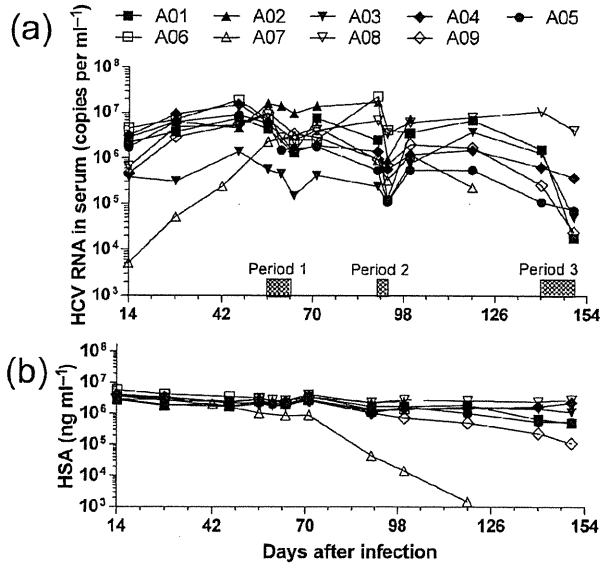

Fig. 1. Lifelong changes in serum HCV RNA and HSA in the blood of HCV-infected mice in the preliminary dose-finding experiment. Nine HCV-infected mice (A01–A09) were treated with telaprevir over three independent periods. The mice were treated with 10 mg telaprevir kg^{-1}, 100 mg telaprevir kg^{-1} or vehicle BID for 7 days (period 1), TID for 3 days (period 2) and TID for 10 days (period 3). (a) Kinetics of serum HCV RNA. (b) Kinetics of HSA level in blood. Because the HSA level indicated the stability of engrafted human hepatocytes in the mice, mouse A07 was excluded from the summary of the results in Table 1.

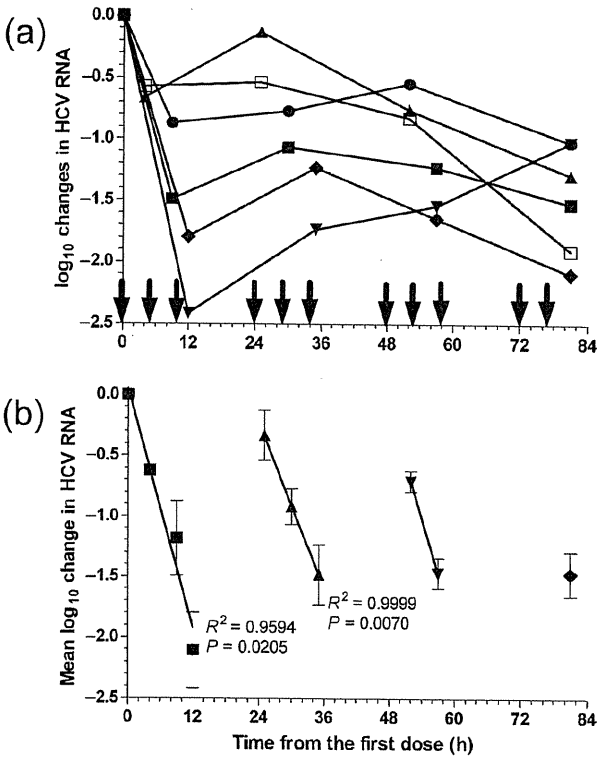

Fig. 2. Estimation of virus clearance rate. Six HCV-infected mice were treated with 200 mg telaprevir kg^{-1} TID for 4 days. Individual kinetics of $\log_{10}$ reductions in serum HCV RNA (a) and of mean $\log_{10}$ changes (±SEM) at each sampling time (b) are represented. Arrows indicate the times of dosing. The slopes of mean $\log_{10}$ HCV RNA reduction were estimated by linear regression analysis. P and R^2 values are indicated on the figure.

reverted back towards baseline levels during the 14 h intermission from drug treatment.

PK analysis

To assess drug exposure after repeated dosing in this mouse model, mice were administered 100 or 300 mg telaprevir kg^{-1} BID for 4 days. The mice receiving 300 mg kg^{-1} BID for 4 days had a mean 2 $\log_{10}$-fold HCV reduction, whereas those receiving 100 mg kg^{-1} BID had up to a 1.5 $\log_{10}$-fold reduction by day 3 (Fig. 3a). Plasma telaprevir concentrations after administration of the final dose are indicated in Fig. 3(b). The estimated half-life of telaprevir in the 100 and 300 mg kg^{-1} groups was 2.4 and 3.8 h, respectively.

PK/PD analysis and the dose-dependent reduction in HCV RNA

To evaluate the correlation between telaprevir concentration and HCV reductions in this mouse model, we used another cohort of 12 HCV-infected mice with high viral loads (1.6×10^6–3.9×10^8 copies ml^{-1}). In this crossover study, mice were randomized into three groups (n=4 each), each of which underwent two periods of dosing for 5 days separated by a 1-week washout period. Serum and plasma samples were collected once daily 5 h after dosing. The mean $\log_{10}$ changes in HCV RNA (±SEM) at different dose levels were calculated from the combined results of both periods (Fig. 4a). The mean $\log_{10}$ reductions from baseline in the 100 and 300 mg kg^{-1} groups were approximately 1 $\log_{10}$ and 1.5–2 $\log_{10}$, respectively, and the difference between the two groups was statistically significant. The means calculated in each period separately are also shown in Fig. 4(b). The plasma telaprevir concentration was positively correlated with the $\log_{10}$ HCV RNA reduction level in each period (Fig. 4c).

Drug concentrations and HCV levels in blood correlate with those in the liver

The correlation between telaprevir concentrations in the plasma and liver was analysed in a double logarithmic plot 5 (dose-finding cohort) or 8 h (PK and PK/PD cohorts) after the last dose (Fig. 5). The linear regression lines suggested that telaprevir concentrations in the liver were 5–

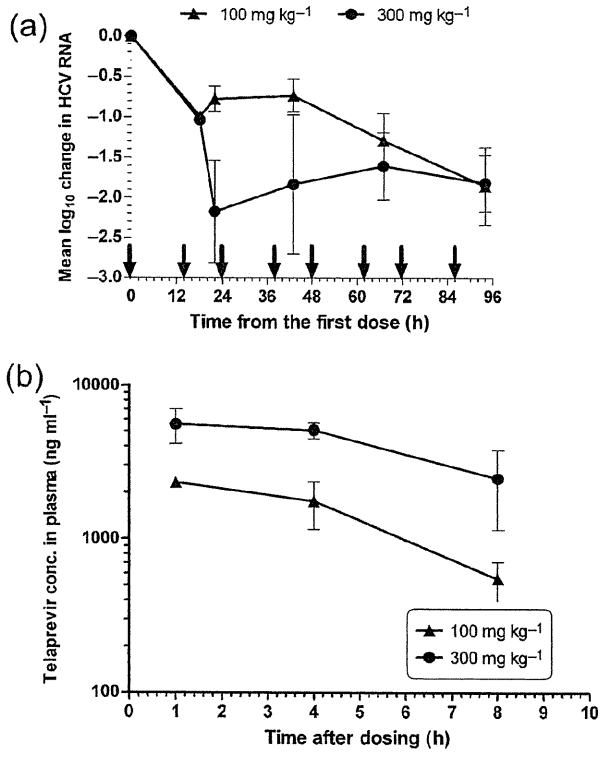

Fig. 3. PK analysis of telaprevir in the HCV-infected mouse model. Six HCV-infected mice were administered 100 (n=3) or 300 (n=3) mg telaprevir kg^{-1} BID for 4 days and serum samples were collected once daily to assess antiviral activity. After the last dose, plasma samples were collected at 1, 4 and 8 h for PK analysis. (a) Mean $\log_{10}$ changes (± SEM) in serum HCV RNA from mice treated with telaprevir. Arrows indicate the times of dosing. (b) Kinetics of telaprevir concentrations in plasma after the last dose.

10-fold higher at 5 h and approximately fourfold higher at 8 h than those in plasma. Total cellular RNA samples were extracted from two, one and four discrete small sections (approx. 50 mg) of the liver in the preliminary dose-finding, PK and PK/PD cohorts, respectively. HCV RNA levels in the total cellular RNA extract were relatively quantified by duplex real-time RT-PCR analysis using human β_2-microglobulin (hβ_2m) as an internal standard of human endogenous gene expression. Neither the threshold cycle (Ct) of hβ_2m ($Ct_{h\beta 2m}$) nor the Ct of HCV (Ct_{HCV}) correlated with total RNA from a small section of the chimeric human livers (data not shown). This result indicated that occupancy rates of human cells varied individually and/or among small sections of the chimeric human liver. Therefore, the mean difference in Ct ($\Delta Ct = Ct_{HCV} - Ct_{h\beta 2m}$) in each mouse was calculated and plotted against the viral load in serum (Fig. 6). After treatment with telaprevir for up to 10 days, mean ΔCt values ranged between 11 (HCV RNA content: $2^{11} = 2 \times 10^3$-fold lower than hβ_2m expression) and 17 (1×10^5-fold lower) among the HCV-infected mice and correlated linearly with $\log_{10}$ serum HCV RNA levels.

Viral dynamics model analysis

To evaluate time-dependent reductions in HCV with BID dosing, 12 HCV-infected elderly mice, which maintained high and steady-state viral loads (1.2×10^6–8.5×10^7 copies ml^{-1}) for more than 6 months, were treated with 200 mg telaprevir kg^{-1} BID for 3 days. The mice were divided into two groups, and serum samples were collected just before the second dose and 4 (n=6) or 8 (n=6) h after every two administrations. The single administration of telaprevir resulted in a mean 0.8–1.0 $\log_{10}$-fold reduction in HCV RNA in both groups. After the second dose, the pattern of viral kinetics appeared to depend on the time of serum collection, and the mean HCV RNA reduction level was higher in the 8 h group than in the 4 h group and plateaued at approximately a 2 $\log_{10}$-fold reduction in both groups after treatment for 3 days (Fig. 7). Finally, we attempted to estimate parameters of efficacy (ε) and virus clearance (c) per hour in this mouse model for comparison with estimates derived from human studies. Because the mean viral kinetics of the 8 h group was biphasic, the values in the 8 h group were used together for the mathematical model analysis. The estimated ε and c values were 0.992 (95 % CI 0.982–1.00) and 0.200 (95 % CI 0.110–0.291), respectively.

DISCUSSION

Using a mouse model with a chimeric human liver for HCV infection, we analysed the PK/PD of telaprevir treatment and investigated HCV dynamics during the initial phase of protease inhibitor treatment. All the mice in this study were expected to have more than half of their livers repopulated by human hepatocytes (Tateno *et al.*, 2004), which simulates a human drug metabolism profile (Katoh *et al.*, 2007, 2008). After the infection with HCV genotype 1b, high viral loads were maintained in the mice for more than 6 months. Recent studies have indicated the utility of a human/mouse chimera model for HCV infection to evaluate antiviral efficacy (Kneteman *et al.*, 2006, 2009) and preclinical safety (Vanwolleghem *et al.*, 2007). However, PK/PD studies and estimations of virus clearance rate have rarely been performed in this mouse model. HCV production, including intracellular replication in engrafted hepatocytes, has also not yet been elucidated. Despite the SCID nature of this mouse model, a 2 $\log_{10}$-fold HCV RNA reduction was observed within 0.5 days, as has been observed previously in CHC patients (Forestier *et al.*, 2007; Reesink *et al.*, 2006). In this mouse model, the rapid rebound in HCV load during the intermission from drug exposure indicated the rapid production and release of HCV into the circulation. This finding indicates that a virion-clearing compartment, which does not depend on T- and B-cell responses, may exist in this mouse model.

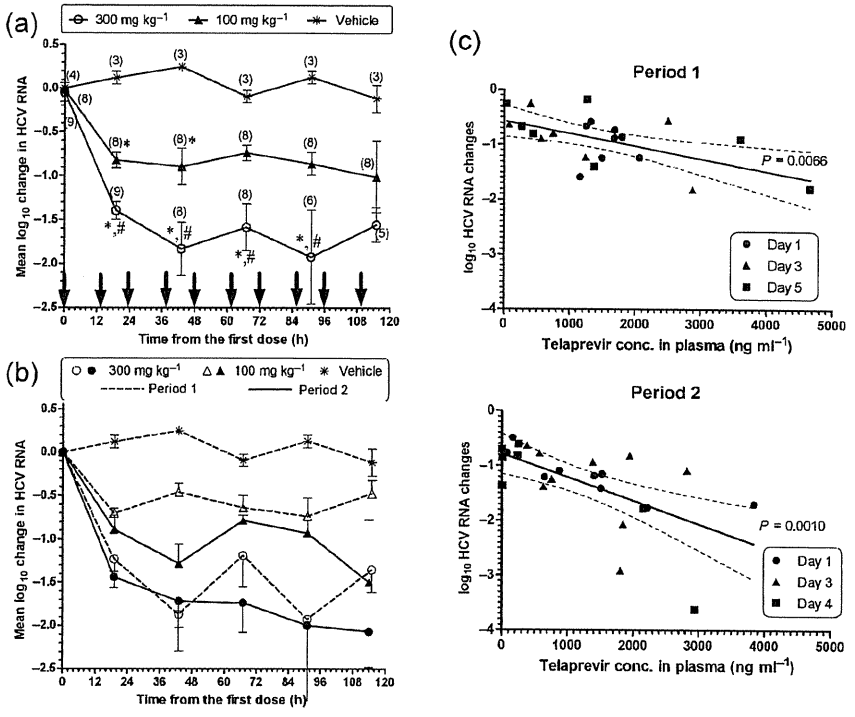

Fig. 4. PK/PD analysis and the dose-dependent reduction in HCV. Twelve HCV-infected mice were randomized into three groups (n=4 each) and then underwent two periods of telaprevir BID dosing for 5 days, separated by a 1-week washout period. Before the second period, the mice in the vehicle control group were additionally assigned to active drug groups. During the second period, mice that received the high or low doses were crossed over to the alternative treatment. Serum and plasma samples were collected once daily 5 h after dosing. Mean $\log_{10}$ changes (±SEM) in serum HCV RNA were calculated from the combined results from both periods (a) and each period separately (b). Arrows indicate the times of dosing. *, $P<0.05$ versus vehicle control group; #, $P<0.05$ versus 100 mg kg^{-1} group. (c) Correlation between $\log_{10}$ reduction in serum HCV and telaprevir concentrations in plasma. Linear regressions (solid lines) and 95% CI (dashed lines) are indicated.

One possible explanation is that viral kinetics after liver transplantation in humans may play a role in HCV clearance under immunosuppressed conditions (Dahari *et al.*, 2005; Powers *et al.*, 2006; Schiano *et al.*, 2005). This observation suggests that this mouse model is capable of evaluating 'first-phase' HCV clearance after drug treatment.

In a clinical trial of telaprevir, CHC patients who exhibited a continuous decline in viral kinetics had mean plasma trough levels above 1000 ng ml^{-1}; therefore, a dose of 750 mg TID was selected for further clinical studies (Sarrazin *et al.*, 2007). When HCV-infected mice were administered 100 or 300 mg telaprevir kg^{-1}, a plasma concentration above 1000 ng ml^{-1} was maintained beyond 8 h in mice treated with 300 mg kg^{-1} but not in those treated with 100 mg kg^{-1}. This result suggests that the extrapolation of telaprevir doses from this mouse model to human studies depends on body surface area, i.e. approximately 15th of a dose in this mouse model may be equivalent to a dose in humans. In another cohort of mice treated with 100 and 300 mg telaprevir kg^{-1} BID, a dose-dependent reduction in HCV was observed and the plasma telaprevir concentration correlated significantly with the HCV reduction level. Therefore, the PK/PD results in this mouse model may be able to indicate a targeted dose range in clinical studies.

Whereas a telaprevir concentration in plasma equivalent to its dosage in clinical trials was achieved in this mouse model, the serum HCV RNA level plateaued at a decrease of approximately 2 $\log_{10}$-fold within several days of treatment. A saturated reduction of approximately 2 $\log_{10}$-fold after treatments with BILN 2061 and IFN was also reported in an analogous mouse model (Kneteman *et al.*, 2006; Vanwolleghem *et al.*, 2007). These observations led us to examine HCV replication in the chimeric human liver. In the relative quantification of HCV RNA against human-specific endogenous gene expression, we observed a correlation between the serum HCV RNA level and the mean ΔCt value in the liver, despite no correlation between the total RNA concentration and each Ct value of two target genes in the liver RNA extracts. This result can be interpreted to indicate that HCV replicated only in

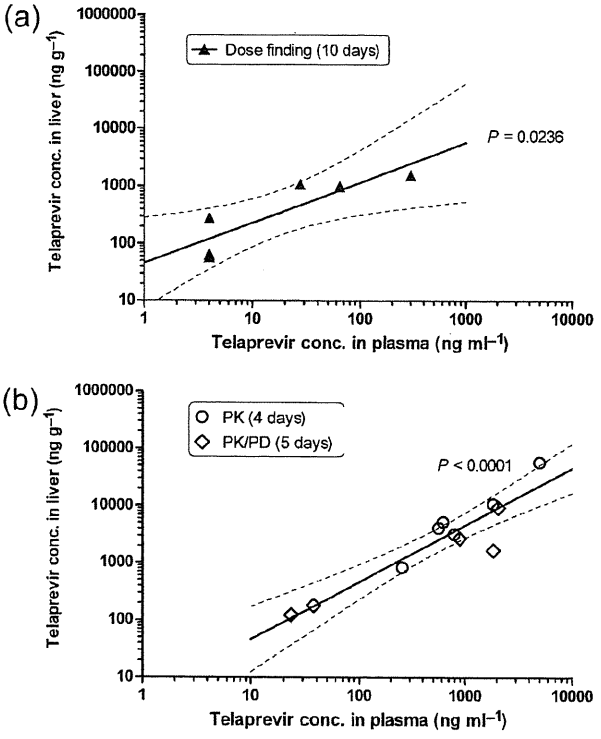

Fig. 5. Correlation between telaprevir concentrations in the liver and plasma. Telaprevir concentrations in the liver and plasma were determined at the end of the three different experiments indicated in Fig. 1 (dose-finding), Fig. 3 (PK) and Fig. 4 (PK/PD). Telaprevir concentrations in the liver were plotted against those in plasma 5 (a) or 8 (b) h after the last dose. Linear regressions (solid lines) and 95 % CI (dashed lines) are indicated.

engrafted human hepatocytes, and the observed HCV reduction in serum might reflect virus replication in the human hepatocyte grafts. Moreover, the relative content of HCV RNA was 2×10^3–1×10^5-fold lower than hβ_2m expression, whereas an HCV replicon cell line, which had approximately 1000 replicon genomes per cell (Quinkert *et al.*, 2005), contained nearly equal amounts of both genes (data not shown). HCV replication was much lower in the engrafted human hepatocytes than in an HCV replicon cell line, and HCV infected only a small portion of the engrafted human hepatocytes. It has been reported that 4–25 % of hepatocytes in a CHC patient were positive for replicative-intermediate RNA, and the mean number of viral genomes per productively infected hepatocyte ranged from 7 to 64 molecules (Chang *et al.*, 2003). Also, a more recent report suggested that the percentage of HCV antigen-positive hepatocytes in patients varied from 0 to 40 %, and the HCV content in 2000 microdissected HCV-positive cells ranged from 40 to 1800 international units using a branched DNA assay (Vona *et al.*, 2004). Therefore, we suggest that HCV replication efficiency in engrafted human hepatocytes is equivalent to that in CHC patients.

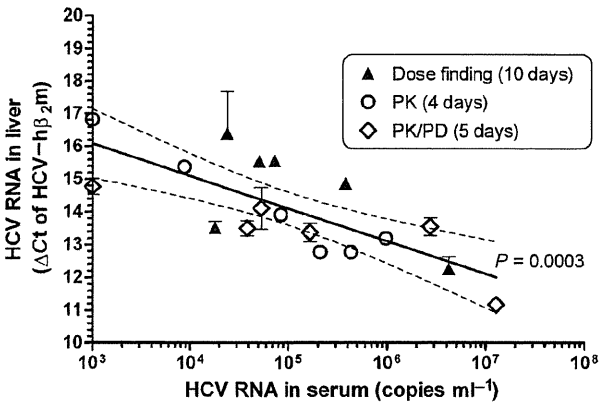

Fig. 6. Correlation between HCV content in the liver and serum. Relative quantification of HCV RNA levels in the liver was determined by the difference between threshold cycles (ΔCt) of HCV RNA and hβ_2m in a duplex real-time RT-PCR analysis. Linear regressions (solid line) and 95 % CI (dashed lines) are indicated.

The differences observed between the engrafted human hepatocytes and the HCV replicon cell line can be explained by the following assumptions: approximately 10 % of engrafted human hepatocytes are productively

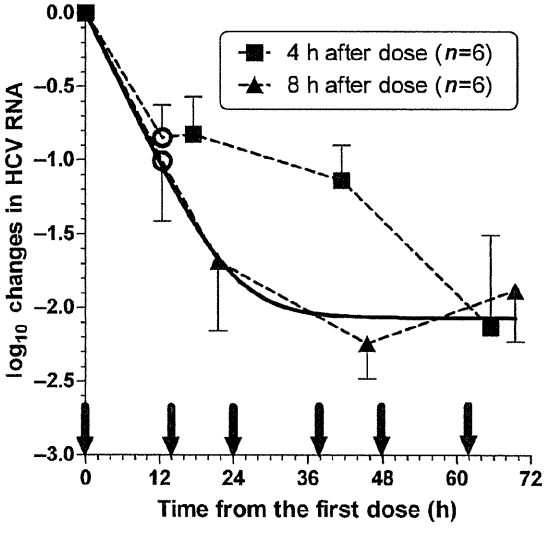

Fig. 7. Viral dynamics under BID telaprevir treatment. Mice were administered 200 mg telaprevir kg^{-1} BID at the times indicated by arrows. Serum samples were collected just before the second dose was administered and 4 (n=6) or 8 (n=6) h after every two doses were administered. Mean $\log_{10}$ changes (±SEM) in serum HCV RNA are plotted. The solved equation described in Methods was fitted to the values in the 8 h group (solid line), and the estimated efficacy and virion clearance rates were 0.992 (95 % CI 0.982–1.00) and 0.200 (95 % CI 0.110–0.291), respectively.

infected and harbour approximately ten HCV genomes per cell at baseline steady state and a 2 $\log_{10}$-fold reduction is achieved with drug treatment.

Mathematical models have proven valuable in understanding the *in vivo* dynamics of HCV, and very rapid dynamic processes occur on timescales of hours to days, and slower processes occur on timescales of weeks to months (Perelson & Ribeiro, 2008). In the last experiment, we observed a biphasic decline in the HCV RNA level after BID dosing for 3 days. During the first 2 days of the treatment, a discrepancy in viral kinetics between the serum-sampling time points was noted. Similarly, fluctuations in viral kinetics during the first-phase slope were observed in patients who received IFN three times a week (Pawlotsky *et al.*, 2004). Variable efficacy rate determined by PK parameters can explain fluctuations during the first-phase slope in mathematical model analysis (Talal *et al.*, 2006). However, it is difficult to evaluate the individual temporal changes in viral and drug kinetics using a mouse model as only a limited volume of blood is available for analysis. Therefore, we assumed a constant efficacy rate (ε) and omitted a turnover rate of hepatocytes because of the short duration of treatment. The estimated clearance rate (c) in this study was 4.8 day^{-1}. Additionally, the mean slope of 0.144 $\log_{10}$ h^{-1} (Fig. 2b) could be transformed to 0.332 h^{-1}=8.0 day^{-1} according to the change of base of a logarithm. The estimated clearance rates in this mouse model basically agreed with estimates determined in humans infected with HCV genotype 1 and undergoing IFN-based therapies (Herrmann *et al.*, 2003; Neumann *et al.*, 1998; Pawlotsky *et al.*, 2004) or large-volume plasma apheresis (Ramratnam *et al.*, 1999). Total virion production during steady-state viral kinetics in this mouse model was calculated by multiplying c by the initial viral load (V_0) and then normalizing the extracellular fluid volume. From previous studies, it was determined that 10^{11}–10^{13} virions are produced daily in patients with high HCV loads (Neumann *et al.*, 1998; Ramratnam *et al.*, 1999). In this mouse model, the volume of extracellular fluid and weight of the liver were approximately 20 and 9% of the body weight (data not shown), and the mean $\log_{10}$ V_0 ($\pm$SEM) among the mice with mean clearance rates of 4.8 and 8.0 per day were 6.96$\pm$0.26 and 7.00$\pm$0.33, respectively. The results of the calculations indicated that 1 g of the chimeric human liver produced 1×10^8–2×10^8 virions per day. The typical weight of the human liver is 1–2 kg; thus, the capacity of human hepatocytes to produce HCV in this mouse model may be equivalent to that in CHC patients. In conclusion, a mouse model with a chimeric human liver can simulate HCV replication in human patients quantitatively and dynamically, and this mouse model may be suitable for preclinical evaluations of novel HCV-specific agents and other therapeutic strategies, including combination regimens.

METHODS

Generation of mice with chimeric human livers and HCV infection. The generation of $uPA^{+/+}/SCID^{+/+}$ mice and transplantation of frozen human hepatocytes was performed at PhoenixBio. Graft function was monitored on the basis of HSA levels in blood (Tsuge *et al.*, 2005). All the mice had high HSA levels, which suggested that nearly half of their livers were repopulated by human hepatocytes (Tateno *et al.*, 2004). After obtaining written informed consent, we collected sera periodically from patients who were chronically infected with HCV genotype 1b and failed to respond to PEG-IFN and RBV therapy. The mice were inoculated with the serum samples via the orbital vein after anaesthetization. The experimental protocol was approved by the Ethics Review Committee for Animal Experimentation of the Graduate School of Biomedical Sciences, Hiroshima University.

Compound preparation and experimental designs. The telaprevir formulations were kindly provided by Vertex Pharmaceuticals. A telaprevir suspension was prepared as described previously (Perni *et al.*, 2006) and used in experiments 1 and 2. In the other experiments, a telaprevir suspension was prepared daily as in the tablet formulation (Forestier *et al.*, 2007; Hézode *et al.*, 2009; McHutchison *et al.*, 2009). A suspension of telaprevir was administered via oral gavage.

Experiment 1: preliminary dose-finding study. Ten out of 11 mice developed serum HCV loads greater than 10^4 copies ml^{-1}. Nine mice with high viral loads (>10^5 copies ml^{-1}) were randomized and administered 10 or 100 mg telaprevir kg^{-1} BID or TID over three periods. During period 1, the mice were administered 100 (n=4) or 10 (n=4) mg telaprevir kg^{-1} or vehicle (n=1) BID at 18:00 and 10:00 h for 7 days, and serum samples were collected before treatment and 1 h after administration in the morning on the third and/or seventh day. During period 2, the mice were administered 100 (n=5) or 10 (n=4) mg telaprevir kg^{-1} TID for 3 days, and serum samples were collected before treatment and 4 h after administration of the last dose. Three mice died between periods 2 and 3. During period 3, the mice were administered 100 (n=3) or 10 (n=3) mg telaprevir kg^{-1} TID for 10 days. The mice were sacrificed 5 h after administration of the last dose, and plasma, serum and liver samples were collected.

Experiment 2: evaluation of HCV turnover. Eleven mice were infected with HCV and eight mice survived for more than 15 weeks with steady-state and high viral loads (10^6–10^8 copies ml^{-1}). Six of the mice were administered 200 mg telaprevir kg^{-1} TID at 9:00, 14:00 and 19:00 h for 4 days. On day 1, serum samples were collected before dose administration, 4 h after the first and second doses were administered, and 2 h after the third dose was administered (n=2 each). On day 2, serum samples were collected 1 h after each of the three doses was administered (n=2 each). Serum samples were also collected 4 h after the first and second doses were administered on day 3 (n=3 each) and 4 h after the second dose was administered on day 4.

Experiment 3: PK analysis. After a washout period, six mice from experiment 2 were administered 100 or 300 mg telaprevir kg^{-1} (n=3 each) BID at 19:00 and 9:00 h for 4 days. Serum samples were collected before dose administration, 4 (n=1) or 8 (n=2) h after administration of the second dose, and 5 h after every two doses were administered. After the final dose was administered, plasma for PK analysis was collected at 1 and 4 h. The mice were sacrificed at 8 h, and serum, plasma and liver samples were collected.

Experiment 4: dose dependence and PK/PD analysis. Thirty-six mice were infected with HCV and 13 survived for more than 13 weeks. The median survival time of this cohort was 81 days after infection. Twelve HCV-infected mice were randomized into three groups (A–C; n=4 each) and underwent two periods of BID dosing for 5 days, which were separated by 1-week washout periods. During the first period, the mice in groups A, B and C were administered 300 mg telaprevir kg^{-1}, 100 mg telaprevir kg^{-1} and vehicle,

respectively. Because two mice in group A and two mice in group C died before the second period, two remaining mice in group C and one back-up mouse were assigned to group A (n=2) and group B (n=1). During the second period, mice that received high or low doses were crossed over to the alternative treatment. Serum samples were collected before the first dose was administered and 5 h after every two doses were administered. Plasma samples were also collected at the same time on days 1, 3 and 5 in the first period and days 1, 3 and 4 in the second period. The mice were sacrificed 8 h after administration of the final dose, and serum, plasma and liver samples were collected.

Experiment 5: viral kinetics with BID dosing After infection of 45 mice, 12 HCV-infected mice maintained steady-state and high viral loads (1.2×10^6–8.5×10^7 copies ml^{-1}) for more than 6 months. The median survival time of this cohort was 131 days after infection. These mice were treated with 200 mg telaprevir kg^{-1} BID at 19:00 and 9:00 h for 3 days. The mice were divided into two groups and serum samples were collected just before the second dose was administered and 4 (n=6) or 8 (n=6) h after every two doses were administered.

Serum RNA extraction and HCV RNA quantification. HCV RNA was isolated from 10 µl serum under denaturing conditions using a SepaGene RV-R kit (Sanko Junyaku). The dried precipitates were dissolved in 10 µl diethylpyrocarbonate-treated water. Extracts were duplicated and assayed by quantitative real-time RT-PCR using TaqMan EZ RT-PCR core reagents (Applied Biosystems). Nucleotide positions of the probe and primer sets refer to HCV H77 strain (GenBank accession no. AF009606). The TaqMan probe 5′-6-FAM-CTGCGGAACCGGTGAGTACAC-BHQ-1-3′ (nt 148–168) was purchased from Biosearch Technologies, and the forward (5′-CGGGAGAGCCATAGTGG-3′; nt 130–146) and reverse (5′-AGTACCACAAGGCCTTTCG-3′; nt 272–290) primers were purchased from Sigma-Aldrich. The 25 µl RT-PCR mixture contained 0.2 nmol forward and reverse primers ml^{-1}, 0.3 nmol TaqMan probe ml^{-1} and 5 µl extracted RNA, and was monitored using a PRISM 7900HT sequence detection system (Applied Biosystems). The thermal profile was 2 min at 50 °C, 30 min at 60 °C for reverse transcription and 5 min at 95 °C, followed by 45 cycles of 20 s at 95 °C and 1 min at 62 °C. The HCV replicon I_{389}neo/NS3-3′/5.1 (Lohmann *et al.*, 1999) RNA was transcribed *in vitro* using a T7 RiboMax Express Large Scale RNA Production System (Promega) and purified twice using gel filtration. The concentration of this transcribed RNA was determined by absorbance at 260 nm and serially diluted 10-fold to prepare a standard curve for each assay.

Liver RNA extraction and HCV RNA quantification. A Wizard SV total RNA Isolation System (Promega) was used to obtain a DNase I-treated total RNA sample. The total RNA concentration was determined by absorbance at 260 nm. Total RNA samples were assayed by duplex real-time RT-PCR for relative quantification of HCV RNA using endogenous control gene expression of human β_2-microglobulin (hβ_2m; GenBank accession no. NM_004048), the TaqMan probe 5′-CAL Fluor Orange 560-AGTGGGATCG-AGACATGTAAGCAGCATCAT-BHQ-1-3′ (nt 401–430), and the forward and reverse primer set of 5′-TTGTCACAGCCCAA-GATAGTT-3′ (nt 379–399) and 5′-TGCGGCATCTTCAAACC-3′ (nt 434–450). To adjust the efficacy of PCR amplification of both target genes, the reaction condition was modified from the HCV single-probe assay. The temperature for extension was 60 °C, the concentration of the HCV probe was 0.24 nmol ml^{-1} and the reaction mixture contained the TaqMan probe/primer set for hβ_2m: 0.2 nmol primers ml^{-1} and 0.12 nmol TaqMan probe ml^{-1}. Because both target genes double after one cycle of PCR, a difference in Ct between HCV and hβ2m ($\Delta Ct = Ct_{HCV} - Ct_{h\beta2m}$) theoretically indicates a relative quantity of HCV RNA per control gene expression of $2^{-\Delta\Delta Ct}$.

Determination of drug concentration. Plasma and liver samples were analysed using chiral liquid chromatography followed by tandem mass spectrometry. After reconstitution, sample extracts were separated by normal-phase chromatography on a 2×250 mm Hypersil CPS-1 column (Thermo Hypersil-Keystone) with a mobile phase of heptane:acetone:methanol (82:17:1). Analyte concentrations were determined by turbo ion spray liquid chromatography/tandem mass spectrometry in the positive-ion mode. Analysis was performed at SRL or Mitsubishi Chemical Medience.

Statistical analysis. The HCV RNA level in serum was normalized by logarithmic conversion. Statistical analysis was performed with a mixed linear model using SAS (SAS Institute). Mean differences between two groups were evaluated with Student's t-test. The difference compared with vehicle control at each time point was evaluated by Dunnett's multiple comparisons test. Linear and non-linear regression analyses were performed using GraphPad Prism 5 (GraphPad Software).

Viral dynamics model analysis. The basic mathematical model for the analysis of HCV infection *in vivo*, which is a system of three ordinary differential equations for uninfected cells (T), productively infected cells (I) and free virus (V), has been reviewed elsewhere (Perelson & Ribeiro, 2008). Briefly, one of the three equations ($dV/dt = pI - cV$), where viral particles are produced at rate p per infected cell and cleared at rate c per virion, was solved. During treatment for 2–3 days, if one assumes that the number of I is approximately constant and equal to its pre-treatment value and that the viral level was at its set-point value (V_0), then $pI = cV_0$. Using this relationship in the equation $dV/dt = (1-\varepsilon)pI - cV$, where ε is the effectiveness in blocking virion production, yields $dV/dt = (1-\varepsilon)\,cV_0 - cV$, $V(0) = V_0$ with the solution $V(t) = V_0(1-\varepsilon+\varepsilon e^{-ct})$. Because the log change of viral load at time [$\log \Delta V(t)$] equals $\log V(t)/V_0$, the solved equation [$\log \Delta V(t) = \log(1-\varepsilon+\varepsilon e^{-ct})$] was fitted to the values obtained in this study via non-linear least-squares regression in order to estimate ε and c.

ACKNOWLEDGEMENTS

We thank Drs Ichimaro Yamada, Mitsubishi Tanabe Pharma Corporation, and Ann D Kwong, Gururaj Kalkeri, Susan Almquist, Steven M. Lyons and John Randle, Vertex Pharmaceuticals, for their thoughtful discussions. This work was supported in part by Grants-in-Aid for scientific research and development from the Ministry of Education, Sports, Culture and Technology and the Ministry of Health, Labour and Welfare, Japan.

REFERENCES

Boonstra, A., van der Laan, L. J. W., Vanwolleghem, T., Harry, L. A. & Janssen, H. L. A. (2009). Experimental models for hepatitis C viral infection. *Hepatology* **50**, 1646–1655.

Chang, M., Williams, O., Mittler, J., Quintanilla, A., Carithers, R. L., Jr, Perkins, J., Corey, L. & Gretch, D. R. (2003). Dynamics of hepatitis C virus replication in human liver. *Am J Pathol* **163**, 433–444.

Dahari, H., Feliu, A., Garcia-Retortillo, M., Forns, X. & Neumann, A. U. (2005). Second hepatitis C replication compartment indicated by viral dynamics during liver transplantation. *J Hepatol* **42**, 491–498.

Forestier, N., Reesink, H. W., Weegink, C. J., McNair, L., Kieffer, T. L., Chu, H.-M., Purdy, S., Jansen, P. L. M. & Zeuzem, S. (2007). Antiviral

activity of telaprevir (VX-950) and peginterferon alfa-2a in patients with hepatitis C. *Hepatology* **46**, 640–648.

Fried, M. W., Shiffman, M., Reddy, K. R., Smith, C., Marinos, G., Gonçales, F. L., Jr, Häussinger, D., Diago, M., Carosi, G. & other authors (2002). Peginterferon alfa-2a plus ribavirin for chronic hepatitis C virus infection. *N Engl J Med* **347**, 975–982.

Herrmann, E., Lee, J.-H., Marinos, G., Modi, M. & Zeuzem, S. (2003). Effect of ribavirin on hepatitis C viral kinetics in patients treated with pegylated interferon. *Hepatology* **37**, 1351–1358.

Hézode, C., Forestier, N., Dusheiko, G., Ferenci, P., Pol, S., Goeser, T., Bronowicki, M.,, Bourlière, J.-P., Gharakhanian, S. & other authors (2009). Telaprevir and peginterferon with or without ribavirin for chronic HCV infection. *N Engl J Med* **360**, 1839–1850.

Hiraga, N., Imamura, M., Tsuge, M., Noguchi, C., Takahashi, S., Iwao, E., Fujimoto, Y., Abe, H., Maekawa, T. & other authors (2007). Infection of human hepatocyte chimeric mouse with genetically engineered hepatitis C virus and its susceptibility to interferon. *FEBS Lett* **581**, 1983–1987.

Katoh, M., Sawada, T., Soeno, Y., Nakajima, M., Tateno, C., Yoshizato, K. & Yokoi, T. (2007). *In vivo* drug metabolism model for human cytochrome P450 enzyme using chimeric mice with humanized liver. *J Pharm Sci* **96**, 428–437.

Katoh, M., Tateno, C., Yoshizato, K. & Yokoi, T. (2008). Chimeric mice with humanized liver. *Toxicology* **246**, 9–17.

Kimura, T., Imamura, M., Hiraga, N., Hatakeyama, T., Miki, D., Noguchi, C., Mori, N., Tsuge, M., Takahashi, S. & other authors (2008). Establishment of an infectious genotype 1b hepatitis C virus clone in human hepatocyte chimeric mice. *J Gen Virol* **89**, 2108–2113.

Kneteman, N. M., Weiner, A. J., O'Connell, J., Collett, M., Gao, T., Aukerman, L., Kovelsky, R., Ni, Z.-J., Hashash, A. & other authors (2006). Anti-HCV therapies in chimeric *scid*-Alb/uPA mice parallel outcomes in human clinical application. *Hepatology* **43**, 1346–1353.

Kneteman, N. M., Howe, A. Y. M., Gao, T., Lewis, J., Pevear, D., Lund, G., Douglas, D., Mercer, D. F., Tyrrell, D. L. J. & other authors (2009). HCV796: a selective nonstructural protein 5B polymerase inhibitor with potent anti-hepatitis C virus activity *in vitro*, in mice with chimeric human livers, and in humans infected with hepatitis C virus. *Hepatology* **49**, 745–752.

Lauer, G. M. & Walker, B. D. (2001). Hepatitis C virus infection. *N Engl J Med* **345**, 41–52.

Liang, T. J., Rehermann, B., Seeff, L. B. & Hoofnagle, J. H. (2000). Pathogenesis, natural history, treatment and prevention of hepatitis C. *Ann Intern Med* **132**, 296–305.

Lindenbach, B. D., Meuleman, P., Ploss, A., Vanwolleghem, T., Syder, A. J., McKeating, J. A., Lanford, R. E., Feinstone, S. M., Major, M. E. & other authors (2006). Cell culture-grown hepatitis C virus is infectious *in vivo* and can be recultured *in vitro*. *Proc Natl Acad Sci U S A* **103**, 3805–3809.

Lohmann, V., Körner, F., Koch, J., Herian, U., Theilmann, L. & Bartenschlager, R. (1999). Replication of subgenomic hepatitis C virus RNAs in a hepatoma cell line. *Science* **285**, 110–113.

Manns, M. P., McHutchison, J. G., Gordon, S. C., Rustgi, V. K., Shiffman, M., Reindollar, R., Goodman, Z. D., Koury, K., Ling, M.-H. & other authors (2001). Peginterferon alfa-2b plus ribavirin compared with interferon alfa-2b plus ribavirin for initial treatment of chronic hepatitis C: a randomised trial. *Lancet* **358**, 958–965.

Manns, M. P., Foster, G. R., Rockstroh, J. K., Zeuzem, S., Zoulim, F. & Houghton, M. (2007). The way forward in HCV treatment – finding the right path. *Nat Rev Drug Discov* **6**, 991–1000.

McHutchison, J. G., Everson, G. T., Gordon, S. C., Jacobson, I. M., Sulkowski, M., Kauffman, R., McNair, L., Alam, J., Muir, A. J. & other authors (2009). Telaprevir with peginterferon and ribavirin for chronic HCV genotype 1 infection. *N Engl J Med* **360**, 1827–1838.

Mercer, D. F., Schiller, D. E., Elliott, J. F., Douglas, D. N., Hao, C., Rinfret, A., Addison, W. R., Fischer, K. P., Churchill, T. A. & other authors (2001). Hepatitis C virus replication in mice with chimeric human livers. *Nat Med* **7**, 927–933.

Neumann, A. U., Lam, N. P., Dahari, H., Gretch, D. R., Wiley, T. E., Layden, T. J. & Perelson, A. S. (1998). Hepatitis C viral dynamics *in vivo* and the antiviral efficacy of interferon-α therapy. *Science* **282**, 103–107.

Pawlotsky, J.-M., Dahari, H., Neumann, A. U., Hezode, C., Germanidis, G., Lonjon, I., Castera, L. & Dhumeaux, D. (2004). Antiviral action of ribavirin in chronic hepatitis C. *Gastroenterology* **126**, 703–714.

Pereira, A. A. & Jacobson, I. M. (2009). New and experimental therapies for HCV. *Nat Rev Gastroenterol Hepatol* **6**, 403–411.

Perelson, A. S. & Ribeiro, R. M. (2008). Estimating drug efficacy and viral dynamic parameters: HIV and HCV. *Stat Med* **27**, 4647–4657.

Perni, R. B., Almquist, S. J., Byrn, R. A., Chandorkar, G., Chaturvedi, P. R., Courtney, L. F., Decker, C. J., Dinehart, K., Gates, C. A. & other authors (2006). Preclinical profile of VX-950, a potent, selective, and orally bioavailable inhibitor of hepatitis C virus NS3-4A serine protease. *Antimicrob Agents Chemother* **50**, 899–909.

Powers, K. A., Ribeiro, R. M., Patel, K., Pianko, S., Nyberg, L., Pockros, P., Conrad, A. J., McHutchison, J. & Perelson, A. S. (2006). Kinetics of hepatitis C virus reinfection after liver transplantation. *Liver Transpl* **12**, 207–216.

Poynard, T., Yuen, M.-F., Ratziu, V. & Lai, C. L. (2003). Viral hepatitis C. *Lancet* **362**, 2095–2100.

Quinkert, D., Bartenschlager, R. & Lohmann, V. (2005). Quantitative analysis of the hepatitis C virus replication complex. *J Virol* **79**, 13594–13605.

Ramratnam, B., Bonhoeffer, S., Binley, J., Hurley, A., Zhang, L., Mittler, J. E., Minarkowitz, M., Moore, J. P., Perelson, A. S. & Ho, D. D. (1999). Rapid production and clearance of HIV-1 and hepatitis C virus assessed by large volume plasma apheresis. *Lancet* **354**, 1782–1785.

Reesink, H. W., Zeuzem, S., Weegink, C. J., Forestier, N., Vliet, A., van de Wetering de Rooij,, J., McNair, L., Purdy, S., Kauffman, R. & other authors (2006). Rapid decline of viral RNA in hepatitis C patients treated with VX-950: a phase Ib, placebo-controlled, randomized study. *Gastroenterology* **131**, 997–1002.

Sarrazin, C., Kieffer, T. L., Bartels, D., Hanzelka, B., Möh, U., Welker, M., Wincheringer, D., Zhou, Y., Chu, H.-M. & other authors (2007). Dynamic hepatitis C virus genotypic and phenotypic changes in patients treated with the protease inhibitor telaprevir. *Gastroenterology* **132**, 1767–1777.

Schiano, T. D., Gutierrez, J. A., Walewski, J. L., Fiel, M. I., Cheng, B., Bodenheimer, H., Jr, Thung, S. N., Chung, R. T., Schwartz, M. E. & other authors (2005). Accelerated hepatitis C virus kinetics but similar survival rates in recipients of liver grafts from living versus deceased donors. *Hepatology* **42**, 1420–1428.

Sherman, K. E., Fleischer, R., Laessig, K., Murray, J., Tauber, W. & Birnkrant, D. (2007). Development of novel agents for the treatment of chronic hepatitis C infection: summary of the FDA antiviral products advisory committee recommendations. *Hepatology* **46**, 2014–2020.

Talal, A. H., Ribeiro, R. M., Powers, K. A., Grace, M., Cullen, C., Hussain, M., Markatou, M. & Perelson, A. S. (2006). Pharmacodynamics of PEG-IFN α differentiate HIV/HCV coinfected sustained virological responders from nonresponders. *Hepatology* **43**, 943–953.

Tateno, C., Yoshizane, Y., Saito, N., Kataoka, M., Utoh, R., Yamasaki, C., Tachibana, A., Soeno, Y., Asahina, K. & other authors (2004). Near completely humanized liver in mice shows human-type metabolic responses to drugs. *Am J Pathol* **165**, 901–912.

Tsuge, M., Hiraga, N., Takaishi, H., Noguchi, C., Oga, H., Imamura, M., Takahashi, S., Iwao, E., Fujimoto, Y. & other authors (2005). Infection of human hepatocyte chimeric mouse with genetically engineered hepatitis B virus. *Hepatology* **42**, 1046–1054.

Vanwolleghem, T., Meuleman, P., Libbrecht, L., Roskams, T., De Vos, R. & Leroux-Roels, G. (2007). Ultra-rapid cardiotoxicity of the hepatitis C virus protease inhibitor BILN 2061 in the urokinase-type plasminogen activator mouse. *Gastroenterology* **133**, 1144–1155.

Vona, G., Tuveri, R., Delpuech, O., Vallet, A., Canioni, D., Ballardini, G., Trabut, J. B., Le Bail, B., Nalpas, B. & other authors (2004). Intrahepatic hepatitis C virus RNA quantification in microdissected hepatocytes. *J Hepatol* **40**, 682–688.

Wasley, A. & Alter, M. J. (2000). Epidemiology of hepatitis C: geographic differences and temporal trends. *Semin Liver Dis* **20**, 1–16.

Liver support systems as perioperative care in liver transplantation-historical perspective and recent progress in Japan

K. INOUE [1], T. WATANABE [1], H. HIRASAWA [2], M. YOSHIBA [3]

[1]*Department of Gastroenterology Showa University Fujigaoka Hospital Yokohama, Japan*
[2]*Department of Emergency and Critical Care Medicine Chiba University School of Medicine Chiba, Japan*
[3]*Division of Internal Medicine Sempo Tokyo Takanawa Hospital, Tokyo, Japan*

A meta-analysis of the efficacy of artificial liver support (ALS) systems for fulminant hepatic failure (FHF) by the Cochrane Hepato-Biliary Group suggested that all ALS systems previously developed are ineffective for FHF. This supports the view that the only treatment of choice for FHF is immediate liver transplantation. Plasma exchange, in combination with high-volume hemodiafiltration or high-flow continuous hemodiafiltration using large pore membranes, which was excluded from the Cochrane meta-analysis because of the lack of randomized control trials, has become a standard ALS system in Japan. This system is safe, and it efficiently removes more low and middle molecular weight toxic substances than other methods by using a large volume of buffers (more than 200 L per session), resulting in recovery from coma in patients with severe FHF comparable to an ahepatic state. These artificial liver support systems are effective tools for sustaining patients with FHF in a favorable condition until liver function recovers or liver transplantation becomes available.

Key words: **Liver - Liver failure - Hemodiafiltration - Plasma exchange.**

The contribution of liver transplantation has improved the survival rate of fulminant hepatic failure (FHF); however, no liver support devices has improved survival rate for this syndrome. The purpose of artificial liver support (ALS) is to sustain patients with FHF or acute-on-chronic liver failure (ACLF) for long enough for the patient's liver to regenerate and regain its function. In cases where the liver cannot regenerate or is progressively deteriorating, ALS should support liver function until transplantation is successfully performed. If these liver support systems had the capability to sustain patients with FHF in a favorable condition, survival rates would be improved and criteria for liver transplantation would be simpler and more accurate.

The liver plays a central role in metabolism. Therefore, complicated metabolic abnormalities occur in FHF; bleeding as a result of depletion of clotting factors and coma due to the accumulation of neurotoxic metabolites are the two major life-threatening symptoms of FHF. In ALS systems, plasma exchange (PE) aims to replace depleted coagulation

Corresponding author: K. Inoue, MD, PhD, Department of Gastroenterology, Showa University Fujigaoka Hospital, 1-30 Fujigaoka, Aoba-ku, Yokohama 227-8501, Japan.
E-mail: kinoue591205@hotmail.co.jp

TABLE I.—*The ALS and Bal systems ever developed.*

Non-biological
- — Standard renal dialysis
- — Whole Blood Exchange Transfusion (WBET)
- — Plasma Exchange (PE), high-volume PE
- — Hemoperfusion (HP) or plasmaperfusion (PP) through resin or charcoal
- — BioLogic DT
- — Molecular Adsorbent Recycling System (MARS), Prometheus
- — Hemodiafiltration (HDF) using high performance membrane
- — Continuous HDF (CHDF), high flow CHDF

Biological and bioartificial
- — Hemoperfusion (HP) through animal or cadaver liver
- — Bioartificial Liver (BAL)
- — Extracorporeal Liver Assist Device (ELAD)

factors while the others aim to provide detoxification. Bioartificial liver (BAL) support devices typically incorporate cultured hepatocytes in bioreactors which aim to provide all of the essential liver functions.

In 2003 [1] and 2004,[2] the Cochrane Hepato-Biliary Group reported the result of a meta-analysis testing the efficacy of previously developed ALS and BAL systems for managing FHF and acute-on-chronic liver failure. Out of 528 references collected, 473 were excluded because they were duplicated, non-clinical, or irrelevant. Of the remaining 55 papers, 41 were also excluded because they were not randomized control trials (RCTs). Thus, only 14 full papers were included.

The methods of ALS and BAL systems included in the meta-analysis were whole blood exchange transfusion (WBET, 1 trial),[3] charcoal hemoperfusion (HP) (1 trial),[4] PE in combination with charcoal HP (1 trial),[5] Biologic-DT (5 trials),[9-10] Molecular adsorbent recirculating system (MARS) (2 trials) [11, 12] HepatAssist BAL (1 trial),[13] and extracorporeal liver assist device (ELAD) (1 trial).[14] The ALS systems excluded from the meta-analysis because they did not perform RCT were PE including high-volume PE [15] and PE in combination with HDF.[16] Therefore, the meta-analysis did not disprove that these two methods are effective.

As expected from the principally limited potential of pilot-controlled trials conducted for the ALS and BAL systems, meta-analysis by the Cochrane group concluded that although these methods increased the survival rate, they did not affect the survival rate in FHF. The study concluded that additional RCTs were needed before any support system could be recommended for clinical use.

It is generally accepted that promising observational data of medical interventions should be verified by RCTs. However, observational studies are rarely free from bias or confounding factors and outcome of the patients with FHF is easily affected by etiology, patients' age, complications and spontaneous recovery. Therefore, a RCT with a small number of patients is also tainted with bias and confounding factors.

PE and HDF/high-flow CHDF is widely accepted as an effective standard treatment in Japan, and thus it is difficult to perform RCTs to ascertain the efficacy of PE and HDF/CHDF using either standard intensive care or MARS as a control. In clinical practice, the pragmatic approach for decision-making should take into accounts the risks and benefits of the local situation, not those of the ideal situation. To sustain patient that fall into an ahepatic state in an alert condition is the ultimate end-point of ALS. To sustain patients for four weeks seems to be a practical end-point for evaluation of ALS. In recent our cases, 4-week survival was 77% (56/73).

Here, we briefly summarize the history of ALS treatments (Table I), and present effective ALS systems currently in use in Japan.

History of non-biological liver support

The first attempted ALS treatment for FHF was the application of standard renal hemodialysis in 1956.[17] Renal dialysis primarily aims to remove ammonia, but it also removes molecules smaller than 500 Da that are implicated in coma associated with FHF, including amino acids, amines, short-chain fatty acids, phenols, and γ-aminobutyric acid. However, such dialysis was deemed ineffective for the treatment of FHF in 1961.[18]

Whole blood exchange transfusion (WBET), which exchanges 6 000 mL of the

patient's blood with normal donor blood, was introduced in 1958 [19] and prevailed until the 1970s. This method aimed to concomitantly correct the two main abnormalities (clotting factor depletion and coma); however, its effectiveness was discredited by a small scale RCT in 1973.[3]

In 1967 a beneficial effect of PE for FHF was reported.[20] PE was aimed at more efficient correcting the coagulation abnormalities and coma of FHF than WBET, and a significant improvement in survival rates was reported in a case series.[21, 22]

Our own experience with PE treatment for FHF showed an overall survival rate of approximately 30%,[23] and although PE is effective in the replenishment of depleted plasma components, it is of a limited value in the removal of substances with large body pool.[24] The concentrations of most of amino acids were not changed by high-volume PE.[25] Consequently, patients with FHF who are receiving PE seldom bleed, but their coma progressively deepens despite daily exchange. This prompted the idea that combining PE with an adequate method to remove toxic substances with large body pool may provide an improved ALS system.[26] PE alone sometimes causes adverse events such as hypernatremia, metabolic alkalosis and sharp decrease in colloid osmotic pressure; however, PE in combination with CHDF [27] (Figure 1) or HDF [26] can reduce these adverse events.

Attempts have been made since the 1950s to remove toxic substances from patients with FHF by perfusing the patient's blood through adsorbents, with the introduction of HP through resin, which experimentally adsorbs bilirubin and bile acid.[28] However, resin HP showed little clinical effect. Rather, it suffered from poor biocompatibility manifested by severe thrombocytopenia.

In 1974, the King's College group reported a favorable clinical effect of HP through 160 g of coated activated charcoal.[29] At the same time, a Japanese group attempted plasma perfusion (PP) through uncoated charcoal;[30] however, a survival rate as low as 19.2% (5/26) was reported with this method.[31] The problem with charcoal PP was its low biocompatibility, and the induction of disseminated intravascular coagulation (DIC).[32] The King's College group later assessed the effect of their own charcoal HP in a RCT, and reported no significant beneficial effect.[4] The Japanese groups thus discontinued using charcoal PP, and switched to PE as their method of choice for an ALS system.

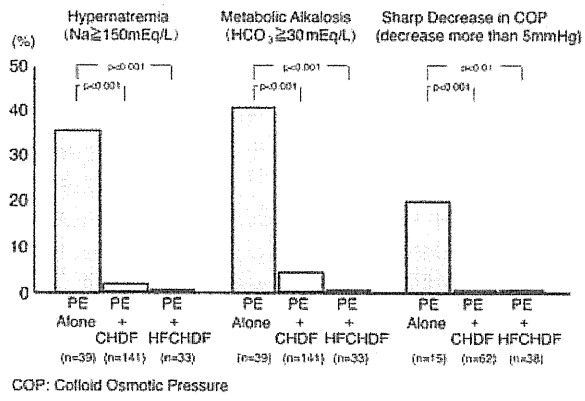

Figure 1.—Incidence of hypernatremia, metabolic alkalosis and sharp decrease in colloid osmotic pressure during ALS treatments. PE: plasma exchange; CHDF: continuous hemodiafiltration; HFCHDF: high flow continuous hemodiafiltration.

The BioLogic-DT system includes a cellulose plate dialyzer with a suspension of powdered activated charcoal and cation exchangers as dialysate.[6] An early study indicated encouraging results in a small trial of ACLF;[9] however, a subsequent study in acute liver failure did not confirm the benefit of this device.[7]

MARS (Teraklin AG, Rostock, Germany) is a closed-loop system that allows passage of albumin-bound toxins up to 50 kDa in diameter to pass from patients' blood to 20% albumin within the circuit. The albumin is then refreshed by passage through charcoal and anion-exchange resin columns. However, there is no evidence that toxins bound to the albumin are effectively delivered to the charcoal and resin. Novelli *et al.* reported 14 patients with acute liver failure successfully supported with MARS before receiving an orthotopic liver transplantation.[33] Tan also reported a beneficial effect of MARS; however, he admitted the necessity of a RCT for MARS.[34] Subsequent RCTs for MARS did not confirm the favorable effect.[11, 12] Prometheus

(Fresenius Medical Care AG, Bad Homburg, Germany) is also a variant of albumin dialysis like MARS removes mainly protein-binding toxic substances. Removal of water-soluble substances is very limited by albumin dialysis as their first step of blood purification.

Instead of perfusing the patient's blood or plasma using adsorbents, other researchers have tried HDF using membranes with larger pores than those used in renal dialysis under the assumption that middle-range molecular substances (MMS) are responsible for the coma in FHF and are not removed by renal dialysis.[35] In 1978 a French group reported a beneficial effect of HDF using polyacrylonitrial (PAN) membrane, which was claimed to be superior in removing MMS than standard kidney dialysis.[36] These findings were not confirmed, however, by a later study,[37] possibly due to the low permeability for MMS of the PAN membrane used in the 1970s.

For the safe and efficient removal of MMS we developed HDF using a larger pore polymethyl metacrylate (PMMA) membrane originally developed for the removal of β2 microglobulin (MW 11 800).[38] The efficacy of this ALS system has been repeatedly reported,[16, 38, 39] and is widely recognized in Japan.[40-42] In the 1990s CHDF using the same PMMA was introduced, and this HDF treatment is used extensively in Japan.[43-46] This technique has been improved by the development of new high performance membranes in Japan.

History of biological and bioartificial liver support

Since Eisman performed HP through porcine liver in patients with chronic liver failure,[47, 48] several attempts have been made to sustain patients with FHF and chronic liver failure by HP through animal [1, 2, 14, 49] and cadaver liver;[5] however, most of these attempts were unsuccessful. Recent developments in tissue engineering have improved cell viability, opening the way for biological liver (BL) and BAL systems that have replaced HP through whole livers.

The HepatAssist BAL uses a column of 300 g of charcoal and 50 g of porcine hepatocytes housed within a hollow fiber bioreactor. Although the BAL was expected to have both synthesis and detoxification capabilities, subsequent clinical trials did not show any favorable effects of the BAL.[15, 45] Xenogenic infections and zoonosis are major drawbacks that hamper use of porcine hepatocyte for BAL.[50, 51]

ELAD uses cells derived from a human hepatoblastoma cell line (C3A) cultured within the extracapillary space of a dialysis cartridge. ELAD is also expected to have both synthesis and detoxification capabilities; however, neither a PCT [14] nor a recent study using a newer version of ELAD [49] demonstrated these features, although they did confirm the safety of ELAD.

In general, bioartificial systems have failed to show any significant benefits in the synthesis of liver-related compounds and have only shown limited detoxifying functions. The first major hurdle for a beneficial BAL support system is to build a bio-component which includes hepatocytes with excellent synthesis and detoxifying abilities, and non-parenchymal liver cells.

Artificial liver support currently prevailing in Japan

The objective of an ALS or BAL systems is to compensate for deficient liver function in liver failure. Therefore, the efficacy of ALS and BAL systems can be judged by assessing to what extent deficient liver function can be compensated. Since the ALS system is a symptomatic treatment for liver failure, the primary end-point of assessment should not be the survival rate, but the potential to completely reverse the symptoms of liver failure in the severest FHF, comparable to an ahepatic state.

Charcoal and resin have been widely used adsorbents and although they have a large capacity to adsorb a wide variety of substances, their capacity is limited when dealing with the accumulation of toxic substances in FHF. For example, the serum level of glutamine, which becomes toxic by releasing

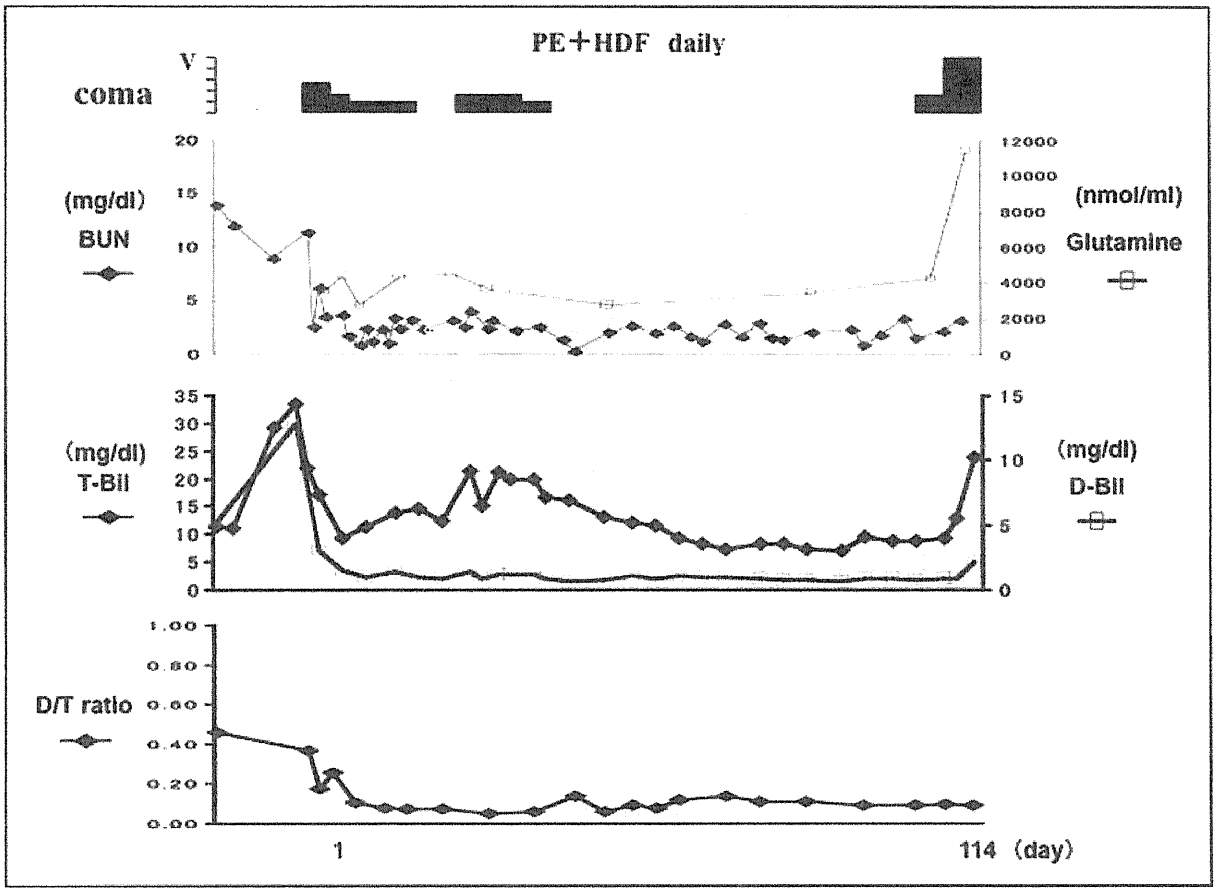

Figure 2.—Clinical course of a 30-year-old female patient with fulminant hepatic failure. Etiology of this case was undetermined. The patient has survived for 114 days under the treatment of artificial liver support consist of plasma exchange and hemodiafiltration using high performance membrane in spite of ahepatic state. Liver weight at autopsy was 210 g.

ammonia, can exceed 10 000 nmol/mL (normal range 422-703 nmol/mL) in a severe case of FHF which is comparable to an ahepatic state (Figure 2). The poor efficiency of BioLogic-DT, MARS, BAL, and ELAD in the removal of toxic substances is illustrated by the poor improvement in encephalopathy shown in the meta-analysis.[2]

PE using high volumes of FFP was shown to be effective for FHF in a number of case studies.[25, 52-56] However, PE using up to 8 L of fresh plasma (high-volume plasma apheresis) is of limited value in removing amino acids such as glutamine with a large body pool.[25] The use of high volumes of plasma is expensive and wastes a limited resource. Therefore, we attempted to remove the MMS as efficiently as possible by an alternative method. We selected high-volume HDF using 70-kDa cut-off PMMA, cellulose triacetate (CTA), and polysulfone (PS), which are three times more efficient in removing inulin than the PAN membrane used by the French group.[56] The HDF removes not only MMS but also lower molecular weight substances such as glutamine effectively.

PE in combination with high-volume HDF as an ALS system has been already established.[35] PE starts with 40 packs (3.2 L) of FFP, which is then adjusted from 20-60 packs to keep the minimum prothrombin time (PT) above 30% of the normal level throughout the treatment course. Hemofiltration starts with 20 L of biocarbonate buffer (Subblood-B, Fuso Pharmaceutical Industries, Ltd., Osaka, Japan) running rapidly for 4 hours. Dialysis is performed concomitantly at a flow rate of 500 mL/min using bicarbonate buffer (Kindaly Solution AF-2, Fuso Pharmaceutical Industries, Ltd., Osaka, Japan). Thus, patient's blood is

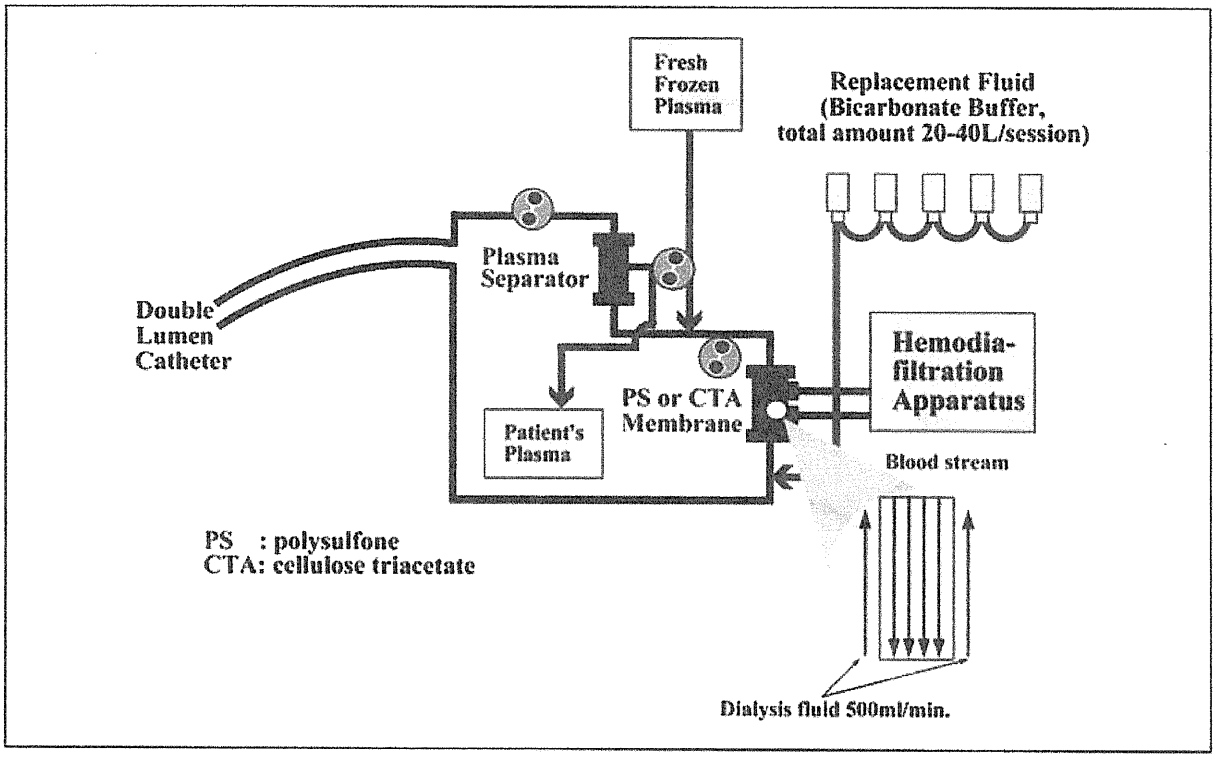

Figure 3.—Circuit diagram for the artificial liver support system currently prevailing in Japan. This system works by plasma exchange using membrane separation and hemodiafiltration with a postdilution method. Flow rate of dialysis buffer is 500 mL/min and volume of filtration buffer is 20-40 L infusing at 5 L/h.

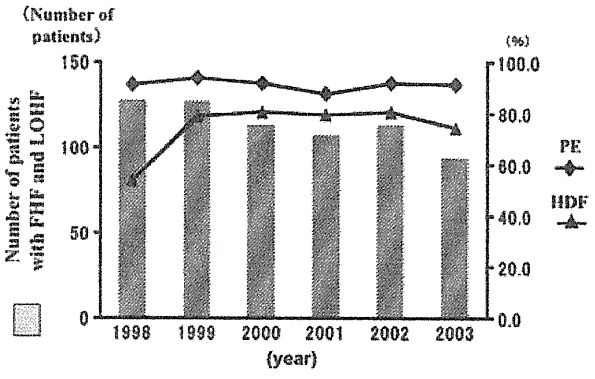

Figure 4.—Number of patients with fulminant hepatic failure and late onset hepatic failure from 1998 to 2003. Use of plasma exchange and hemodiafiltration annually during the period.

cleansed by 170 L of buffer at the start. The volume of filtrate is increased up to 40 L through post-dilution route depending upon the patient's response, and thus the patient blood is cleansed maximally by a significantly large volume of 340 L of buffer per session (Figure 3).

In 1986, we first reported complete recovery from deep coma in a patient with severe FHF caused by hepatic vein obstruction.[26] The efficacy of this ALS system was further substantiated in studies of 27 and 67 patients with FHF, which gave surprisingly high rates of recovery (92.6% and 97%, respectively) from the initial coma.[16, 39] Brain edema and renal failure are observed in 19%, and 11% of cases on admission, respectively and most of the cases recovered. The effectiveness of this ALS system is now widely recognized in Japan.[40-42] Some investigators have modified the rapid HDF to continuous HDF (CHDF) with also good results.[43-46] A national annual surveillance study supported by the Ministry of Health, Welfare and Labor of Japan, which collected data from 1998 to 2003, reported the use of PE and HDF/CHDF in 91.5% (637/696) and 74.6% (519/696) of patients with FHF or late-onset hepatic failure, respectively [57] (Figure 4). Recently, recovery from brain edema in severe FHF was reported using this methods of ALS system.[58] The